Title

Single-fibre proteomics reveals a greater fibre-type specific mitochondrial remodelling with moderate than high-intensity training.

Author list

E. Reisman[1,2,12], J. Botella[1,3,12], C. Huang[4], R. B. Schittenhelm[4], D. A. Stroud[5,6], C. Granata[1,7,8,9], S. Chandrasiri[1], G. Ramm[10], V. Oorschot[10], N. J. Caruana[1,5*] & D. J. Bishop[1*]

Affiliations

1. Institute for Health and Sport (iHeS), Victoria University, Melbourne, Victoria, 3011, Australia
2. Mary MacKillop Institute for Health Research, Australian Catholic University, Melbourne, Victoria, 3000, Australia
3. Metabolic Research Unit, School of Medicine and Institute for Mental and Physical Health and Clinical Translation (IMPACT), Deakin University, Waurn Ponds, Victoria, 3216, Australia.
4. Monash Proteomics & Metabolomics Facility, Biomedicine Discovery Institute and Department of Biochemistry and Molecular Biology, Monash University, Clayton, Victoria, 3168, Australia
5. Department of Biochemistry and Pharmacology, Bio21 Molecular Science and Biotechnology Institute, The University of Melbourne, Parkville, Victoria, 3052, Australia
6. Murdoch Children's Research Institute, Royal Children's Hospital, Parkville, Victoria, 3052, Australia
7. Department of Diabetes, Central Clinical School, Monash University, Melbourne, Victoria, 3004, Australia
8. Institute for Clinical Diabetology, German, Diabetes Center, Leibniz Center for Diabetes Research at Heinrich-Heine-University, Düsseldorf, Düsseldorf, 40225, Germany
9. German Center for Diabetes Research, Partner Düsseldorf, München-Neuherberg, 40225, Germany
10. Ramaciotti Centre for Cryo EM, Biomedicine Discovery Institute and Department of Biochemistry and Molecular Biology, Monash University, Clayton, Victoria, 3168, Australia
11. Electron Microscopy Core Facility, European Molecular Biology Laboratory, Heidelberg, 69117, Germany

12. These authors contributed equally to this work

* Correspondence: David.Bishop@vu.edu.au, nikeisha.caruana@vu.edu.au

Summary

Analyses of mitochondrial adaptations in human skeletal muscle have mostly used whole-muscle samples, where results may be confounded by the presence of a mixture of type I and II muscle fibres. Using our MS-based proteomics workflow, we provide new insights into fibre-specific mitochondrial adaptations following two types of exercise training that were very different in terms of metabolic demands and fibre recruitment patterns – moderate-intensity-continuous training (MICT) and sprint interval training (SIT). There was a larger number of differentially expressed proteins in each fibre type following MICT than SIT. Our novel mitochondrial normalisation strategy highlighted that most training-induced changes in mitochondrial protein abundances were stoichiometrically linked to the overall increase in mitochondrial content, except for the decreased abundance of complex IV subunits in both type I and II fibres following SIT, and the increase in proteins associated with fatty acid oxidation in type I fibres.

Keywords: Proteomics, single fibre, exercise, complex IV, fatty acid oxidation

Introduction

The remarkable ability of skeletal muscle to adapt to repeated contractile stimuli is one of the most fundamental and intriguing aspects of physiology (Egan and Zierath, 2013). Repeated exercise sessions (i.e., exercise training) alter the expression of proteins, which can lead to improved maintenance of cellular homeostasis (Hawley et al., 2014), altered metabolism (Hargreaves and Spriet, 2020), and the prevention and treatment of many chronic diseases (Neufer et al., 2015). Exercise is also a potent stimulus to activate mitochondrial biogenesis (Bishop et al., 2019a; Miller and Hamilton, 2012), with resulting increases in mitochondrial content and respiratory function (Granata et al., 2021; Holloszy and Coyle, 1984). These adaptations appear to depend on the characteristics of the exercise stimulus (Jamnick et al., 2020; MacInnis and Gibala, 2017).

One limitation of most human training studies to date is the analysis of whole-muscle samples, where the results may be confounded by diverse changes in different fibre types (Murphy, 2011). Human skeletal muscle is composed of three major fibre types (type I, IIa, and IIx), which differ in their contractile, metabolic, and bioenergetic characteristics; this is reflected by a greater reliance on mitochondrial oxidative enzyme activity in type I fibres (Howald et al., 1985; Ingjer, 1979; Kiessling et al., 1974) and greater glycolytic enzyme activity in type II fibres (Jackman and Willis, 1996). Furthermore, Henneman's size principle (Henneman and Olson, 1965) proposes that type I fibres have a lower threshold of activation, and will be recruited at lower exercise intensities, whereas fast-twitch fibres (type IIa and IIx) have a higher activation threshold and will be increasingly recruited at greater exercise intensities (Sale, 1987; Vollestad and Blom, 1985). Skeletal muscle fibre recruitment is therefore related to exercise intensity (Sale, 1987; Vollestad and Blom, 1985), and it has been hypothesised that higher exercise intensities might stimulate greater adaptations in type II fibres relative to lower intensities (Henneman, 1957; Henneman and Olson, 1965; Mendell, 2005). It has also been proposed that recruitment of type II fibres may help to explain the greater mitochondrial adaptations reported following high-intensity training (Dudley et al., 1982; MacInnis and Gibala, 2017; Sale, 1987; Vollestad and Blom, 1985). Until recently, however, technical limitations have prevented the direct assessment of fibre-type-specific adaptations to different types of exercise training.

Modifications to immunoblotting protocols have enabled researchers to identify training-induced adaptations of mitochondrial proteins in single skeletal muscle fibres (MacInnis et al., 2017; Skelly et al., 2021; Tan et al., 2018; Wyckelsma et al., 2015). However, due to limited starting material,

only five of the more than 1100 known mitochondrial proteins have been investigated to date (Kristensen et al., 2015; MacInnis *et al.*, 2017; Murphy, 2011; Skelly *et al.*, 2021; Tan *et al.*, 2018; Wyckelsma *et al.*, 2015). Improvements in mass-spectrometry-based proteomic techniques have allowed greater resolution of the contractile and metabolic features of single skeletal muscle fibre types – first in mice (Murgia et al., 2015) and then also in humans (Murgia et al., 2017). The detection of functionally important low-abundance proteins, in addition to thousands of other proteins, was a significant development that has advanced our understanding of the breath and complexity of proteins at the fibre level in skeletal muscle. Recent work has built on this research and adapted this technique to highlight fibre-type-specific protein changes to moderate-intensity continuous training (MICT) in the skeletal muscle of a small number of males (n=5) (Deshmukh et al., 2021). To date, however, no proteomic study has investigated the effects of divergent exercise intensities, which differ in their recruitment of the major fibre types, on fibre-type-specific mitochondrial adaptations. A greater understanding of fibre-type-specific adaptations to different exercise intensities may help to optimise the prescription of exercise to prevent and treat diseases, as well as counteract some of the detrimental effects of ageing.

In the present study, we developed a sensitive mass spectrometry-based (MS) proteomics workflow that allowed for the pooling of single muscle fibres, and the utilisation of tandem mass tag (TMT) labelling, to facilitate the identification of low abundant mitochondrial proteins. To investigate potential fibre-type-specific changes in protein abundances following training, we employed two very different training interventions - MICT and sprint-interval training (SIT). These two types of training were chosen as they differ in intensity (i.e., moderate versus very high intensity) and have been reported to require different skeletal muscle fibre recruitment patterns (Dudley *et al.*, 1982; Kristensen *et al.*, 2015; Suriano et al., 2010). Our findings reveal distinct fibre-type-specific protein responses to these two different types of exercise. Following MICT, changes in proteins (including mitochondrial proteins) were primarily observed in type I fibres. Despite the hypothesis that SIT would target type II fibres, we observed few differentially expressed proteins following SIT. There was, however, a decreased abundance of complex IV subunits in both type I and II fibres following SIT. We also observed that most training-induced changes in mitochondrial protein abundances were stoichiometrically linked to the overall increase in mitochondrial content. Our study provides a new analytical approach that expands our fundamental understanding of fibre-type-specific adaptations to different types of exercise training. These findings challenge and expand our current knowledge of fibre-type-specific changes to mitochondrial proteins in response to exercise training and provide an

important resource that may help to reveal the contribution of fibre-type-specific differences to health and disease.

RESULTS

Single-fibre proteomics

Only two studies in young men, both with small sample sizes (n = 4 and 5, respectively), have employed proteomics to describe fibre-type-specific differences for the contractile and metabolic features of human skeletal muscle fibres (Deshmukh *et al.*, 2021; Murgia *et al.*, 2017). In the present study, twenty-three, recreationally active, healthy men completed one of two 8-week training interventions, consisting of either moderate-intensity continuous training (MICT) or very high-intensity sprint-interval training (SIT) (see Table S1 – Tab 1 for participant characteristics). Pre and post training, skeletal muscle biopsies were collected from the vastus lateralis muscle and single fibres were isolated, fibre-typed, pooled, and analysed utilising the proteomic workflow described in Figure 1a.

One of the challenges of analysing skeletal muscle is the large dynamic range of protein concentrations caused by the highly abundant sarcomeric proteins, which account for over 50% of the total proteome (Deshmukh et al., 2015; Murgia *et al.*, 2015; Ohlendieck, 2010; 2013), while proteins from all other muscle compartments, including the mitochondria, are confined to the lower half of the abundance range (Deshmukh *et al.*, 2015). Compared to typical whole-tissue proteomic studies, single-muscle fibres provide very low protein yields (Galpin et al., 2012; Murgia *et al.*, 2015), which further complicates the identification of lower abundant proteins (Deshmukh *et al.*, 2015; Ohlendieck, 2011). While previous studies have used label-free quantitative shotgun approaches after filter-aided sample preparation (Deshmukh *et al.*, 2021; Murgia *et al.*, 2017), we chose a workflow incorporating tandem mass tag (TMT) labelling, which not only allowed us to increase sample size and throughput to accommodate our complex experimental design but also exhibits higher quantitative precision than label-free quantification (O'Connell et al., 2018; Pappireddi et al., 2019).

Our approach identified a total of 3141 proteins across all pooled samples, with 81% (2534 proteins) of these identified with high confidence (false discovery rate [FDR] < 0.05) and > 1 unique peptide (Table S1-Tab 2). On average, we were able to reliably identify 1857 ± 59 (1477 to 2000) high-confidence proteins per pooled single-fibre sample (Figures S2a, b, & c, Table S1-Tab 2; see also

Table S9 – Tab 1 & Tab 2). Proteins were removed from the dataset if they contained more than 70% missing values, leaving a total dataset across all samples of 1623 proteins (Table S1-Tab 3).

To further understand the characteristics of the fibre-specific proteome, we examined the cellular localisation of the proteins identified in each individual sample of pooled type I or type II fibres based on Gene Ontology Cellular Components (GOCCs). GO enrichment analysis of our dataset (Figure 1b, Table S1-Tab 4) demonstrates good coverage of the structural and metabolic features of the muscle fibre proteome, including contractile, sarcomeric, ribosomal, and mitochondrial proteins.

To assess the comprehensiveness of our protein detection in pooled single fibres, we compared our dataset to the two previous studies (Deshmukh *et al.*, 2021; Murgia *et al.*, 2017) investigating the single muscle fibre proteome in humans (Figure 1c, Table S1-Tab 5). There were 846 proteins in common between the three studies, which may represent proteins that can more confidently be used to compare fibre types in human skeletal muscle. One of the most significantly enriched cellular components for these commonly identified proteins was the mitochondrion (Figure 1d, Table S1-Tab 6).

Fibre Type Differences in the Pre-Training samples

Multi-dimensional scaling revealed a good separation of the protein profiles between type I and type II fibres for most, but not all, pooled single fibre samples expressed between fibre types pre-training (Figure 1e). Although the separation between fibre types was not as distinct as previously reported (Deshmukh *et al.*, 2021), this may reflect the approximately 20% greater aerobic fitness of our participants ($\dot{V}O_{2max}$ = 52 vs ~ 44 $mL \cdot min^{-1} \cdot kg^{-1}$) and previous reports that type II fibres become more like type I fibres with endurance training (Bergh et al., 1978; Jansson et al., 1978; Wilson et al., 2012).

Proteomic features of the different fibre types are presented in a volcano plot (Figure 1f). A total of 120 proteins were identified as differentially expressed between fibre types pre-training (PRE), using an empirical Bayes method and with statistical significance set at an adjusted P value cut-off of 0.05 (Table S1-Tab 7). Our results are in agreement with previous work (Deshmukh *et al.*, 2021), although their study did identify a greater number of differentially expressed proteins between fibre types when they adopted a posteriori information fusion scheme – a statistical approach that combines biological significance (fold change) and statistical significance (P value from a single

paired t-test) (Xiao et al., 2014). Unsupervised hierarchical clustering revealed a clear separation of fibre types, although, as expected, there was some biological variability amongst individuals (Figure 1g).

Our analysis revealed new contractile proteins with fibre-type-specific expression profiles (Table S1-Tab 8). These included MYH3 and MYL4 – two poorly understood members of the myosin family (Schiaffino et al., 2015). We also observed many of the expected differences between fibre types. Type I fibres were characterised by a greater abundance of contractile proteins belonging to the myosin heavy (MYH7) and light (MYL6B) chains, as well as troponin (TNNT1, TNNC1, TNNI1) and an isoform of the sarcoplasmic reticulum Ca^{2+}-ATPase (ATP2A2, also named SERCA2; (Lamboley et al., 2015; Morissette et al., 2014)), while type II fibres possessed a greater abundance of MYH2, MYL1, TNNT3, TNNC2, TNNI2, and also ACTN3.

Most studies on muscle fibre heterogeneity have focused on contractile proteins (Ohlendieck, 2013; Schiaffino, 2011). However, as confirmed in our study, the diversity between muscle fibres is not only restricted to contractile proteins but extends to a wide range of subcellular systems - including ionic transport, cellular calcium signalling, and metabolism (Schiaffino, 2011). Approximately 25% of the proteins identified as differentially expressed between fibre types were mitochondrial – with most (~ 95%) having a greater abundance in type I fibres. These differentially expressed mitochondrial proteins were enriched in pathways associated with fatty acid oxidation, as well as other proteins responsible for the provision and transfer of electrons to support energy provision (Table S1-Tab 7).

Influence of mitochondrial content on fibre-type-specific expression profiles

Of the 395 mitochondrial proteins quantified in the present study, 273 (~ 70%) were in common with the previous two single-fibre proteomic studies (Figure 2a, Table S2-Tab 1). The top 5 GO Biological Process (BP) terms for these commonly detected mitochondrial proteins were related to mitochondrial electron transport (NADH to ubiquinone and respiratory chain complex I assembly), the tricarboxylic acid cycle, fatty acid beta-oxidation, and branched-chain amino acid catabolic processes (Figure 2b, Table S2-Tab 2). In line with their superior capacity for oxidative phosphorylation and fatty acid oxidation (Sahlin et al., 2007), and in agreement with previous work (Deshmukh *et al.*, 2021), we also observed that type I fibres had a significantly greater abundance of many mitochondrial proteins (Figure 2c, Table S1-Tab 7).

An important question that has not been adequately addressed is whether these fibre-type-specific expression profiles for mitochondrial proteins are independent of the greater mitochondrial content in type I versus type IIa human skeletal muscle fibres (Howald *et al.*, 1985; Kiessling et al., 1971; Ørtenblad et al., 2018). To examine the potential influence of mitochondrial content on fibre-type-specific expression profiles for mitochondrial proteins, we first calculated the mitochondrial protein enrichment (MPE) – a value that identifies the contribution of mitochondrial protein intensities to the overall detectable proteome (Granata *et al.*, 2021). Consistent with previous research (Deshmukh *et al.*, 2021), there was a greater abundance of proteins associated with the mitochondria cellular component in type I compared to type II fibres ($P < 0.05$, Figure 2d, Table S2-Tab 5). As this supported an overall greater content of mitochondria in type I versus type II fibres in our participants, we next employed our previously described normalisation strategy (Granata *et al.*, 2021), which corrects for the bias introduced by differences in total mitochondrial content, to identify the relative abundance of individual mitochondrial proteins within each fibre type. This strategy allows us to identify fibre-type differences in mitochondrial protein abundance that are disproportionate to fibre-type differences in the total mitochondrial proteome. Post normalisation, only 8 of the 27 mitochondrial proteins we had previously observed to have fibre-type-specific expression profiles remained significantly different (see Figure 2c and compare Figure 2e, Table S1-Tab 7, with Figure 2f, Table S2-Tab 7). This novel analysis suggests that many of the differences in mitochondrial protein abundances between fibre types reported by us, and others (Deshmukh *et al.*, 2021; Murgia *et al.*, 2017), might be due to differences in total mitochondrial content rather than fibre-type-specific remodelling of the mitochondrial proteome.

Proteomic responses to different types of training in type I and type II skeletal muscle fibres

Skeletal muscle has a remarkable ability to remodel in response to repeated contractile stimuli, but little is known about fibre-type-specific changes in protein abundances following exercise training. To date, only one proteomic study has reported fibre-type-specific adaptations to one type of exercise training (1 h at 75 to 90% of maximum heart rate, 4x/week for 12 weeks) in the skeletal muscle of five males (Deshmukh *et al.*, 2021). However, it is not known if fibre-type-specific changes to the proteome depend on the nature of the exercise stimulus. The size principle states that type I fibres are mostly utilised at lower exercise intensities, whereas type II fibres are increasingly recruited at higher intensities (Henneman and Olson, 1965; Mendell, 2005). Therefore, a long-standing hypothesis is that training-induced changes to the proteome in response to low-intensity

exercise will mostly be confined to the type I fibres that are predominantly recruited with this type of exercise (Godin et al., 2010; Sale, 1987). In contrast, higher-intensity exercise (e.g., all-out sprinting) has been proposed to stimulate greater adaptations in type II fibres compared to exercise performed at lower intensities (Greenhaff et al., 1994).

To investigate fibre-type-specific changes to the proteome in response to divergent exercise stimuli, we had 23 healthy young men train 3 to 4 times per week for 8 weeks after random assignment to one of two very different types of training – MICT or SIT (Figure 3a). By design, both exercise groups had very different exercise prescription characteristics; there was a 4.7-fold greater exercise intensity for SIT and a 5.2-fold greater training volume for MICT (Figure 3b). The divergent exercise prescriptions, and their associated effects on the metabolic response to exercise, can be observed by the large increase in blood lactate concentration following SIT (9.9-fold; 1.6 ± 0.6 to 15.7 ± 5.9 $mmol \cdot L^{-1}$; $P < 0.001$) when compared to MICT (1.6-fold; 1.38 ± 0.43 to 2.18 ± 0.38 $mmol \cdot L^{-1}$; $P = 0.001$) (Figure 3b; Table S3-Tab 1). Similarly, blood pH levels were only decreased following SIT (from 7.35 ± 0.03 to 7.05 ± 0.09; $P < 0.001$) and not MICT (from 7.35 ± 0.02 to 7.37 ± 0.02; $P > 0.05$) (reflected by fold differences in $[H^+]$ in Figure 3b). These results agree with the well-described effect of exercise intensity on increasing glycolytic flux through anaerobic pathways and the associated increase in lactate and decrease in pH (Hargreaves and Spriet, 2020; van Loon et al., 2001). Immunohistochemical analysis of muscle sections confirmed there was a greater depletion of muscle glycogen in type I than type II fibres following the first MICT session, and greater muscle glycogen depletion in the type II fibres following SIT versus MICT (Figure 3c). This is consistent with previous research (Gollnick et al., 1974; Scribbans et al., 2014) and demonstrates that the two different types of training employed were associated with very different skeletal muscle fibre recruitment patterns (i.e., MICT recruited predominantly type I fibres while SIT recruited both type I & type II fibres; Figure 3d).

As with previous research (Deshmukh *et al.*, 2021), to identify fibre-type-specific changes in protein abundances following exercise training we chose a posteriori information fusion scheme that combines biological relevance (fold change) and statistical significance (P value) (Xiao *et al.*, 2014). The fusion scheme yields a protein significance score (π value) and is robust in selecting differentially expressed genes/proteins while protecting against false discoveries. Using this fusion scheme, we identified 31 and 16 proteins that were differentially altered by 8 weeks of MICT in type I and type II fibres, respectively (Figure 4a, b, left panels; Table S4-Tabs 1 & 3), with no overlap between the proteins altered in each fibre type (Figure 4c; Table S4-Tab 5). Many of the proteins

with a lower abundance following MICT in type I fibres were related to skeletal muscle contraction (Table S4-Tab 5). The decrease in the abundance of these proteins following MICT raises the possibility that the fibre-type differences for these contraction-related proteins observed pre-training may be a consequence of habitual physical activity rather than an intrinsic characteristic of the different fibre types. In contrast to our hypothesis, there were few proteins that changed their abundance in either type I or type II fibres following SIT (i.e., 4 to 8 x 30-s all-out sprints performed 3 to 4 times a week for 8 weeks) (Figure 4a,b, right panels; Table S4-Tabs 2 & 4). As with MICT, there was no overlap between the proteins altered in each fibre type following SIT (Figure 4d; Table S4-Tab 6).

The fibre-type-specific adaptations to MICT are strengthened by the greater number of differentially expressed proteins between type I and type II fibres post-training compared to pre-training (compare Figure 5a; Table S5-Tab 1 with Figure 1f). Similarly, the limited effects of SIT on the proteome are reinforced by the small difference in the number of differentially expressed proteins between type I and type II fibres in the SIT group after training versus pre-training (compare Figure 5b; Table S5-Tabs 2 with Figure 1f). There were also far fewer proteins with altered expression in either type I or type II fibres following SIT compared with MICT (Figure 5c; Table S5-Tab 3). Approximately 75% of the proteins identified as differentially expressed between type I and type II fibres following SIT also had fibre-specific differential expression pre-training (Figure 5d; Table S5-Tab 4), further supporting the limited effects of SIT on the proteome. These results are consistent with those from a study that used immunoblotting on pooled single fibres and observed greater fibre-type-specific changes following MICT compared with SIT (Skelly *et al.*, 2021).

Of note, we identified an additional 80 differentially expressed proteins between the two fibre types post-MICT that were not differentially expressed between the two fibre types pre-training (Figure 5d; Table S5-Tab 4). This again suggests greater fibre-type-specific changes to the proteome in response to MICT than SIT. However, only six of these 80 proteins were also identified as being significantly altered by 8 weeks of MICT (CES2, CLIC5, ETFB, LASP1, QDPR, TGM2; Table S4-Tabs 1 & 3). Enrichment analysis was completed on all detected proteins in the POST samples for each fibre type and for each training type (using the WikiPathways database; Figure 5e; Table S5-Tab 5). Several pathways presented differences between fibre types in both directions (i.e., some proteins within a pathway were higher in abundance in type I fibres and some proteins within the same pathway were higher in type II fibres) – including pathways associated with striated muscle contraction and proteasome degradation. Fibre-type-specific pathways included glycolysis and

gluconeogenesis, which had a greater enrichment in type II fibres for both groups. In contrast, the pathways related to fatty acid oxidation and the TCA cycle were more prevalent in type I than type II fibres.

We narrowed the analysis to look specifically at pathways related to muscle contraction, metabolism, and glycolysis, and observed that specific proteins (and pathways) were differentially expressed in the two fibre types after both training interventions (i.e., in MICT and SIT) (Figure5f; Table S5-Tab 6). The network analysis demonstrates that protein differences were more common between the same fibre type than the same exercise training type. For example, for both types of training striated muscle contraction proteins associated with slow-twitch skeletal muscle isoforms were predominately higher post-training in type I fibres (TNNT1, TNNI1, TNNC1, MYL2 and MYL3), while proteins associated with fast-twitch skeletal muscle isoforms were predominately more abundant post-training in type II fibres (TNNC2, MYH6, ACTN3, TNNT3, MYBPC2, TPM1, TNNI2, MYL1 and MYL4). There was also an influence of training type, with the greater abundance of fast-twitch skeletal muscle proteins in type II fibres attributable to a lower abundance of these proteins in type I fibres post MICT and no change in either fibre type post SIT (compare Figure 5f to Figures 4a & 4b). The network analysis also indicated that proteins associated with glycolysis were mostly differentially expressed only in type II fibres after both types of training; proteins belonging to the glycogen synthesis pathway were only observed to be greater in type II fibres post MICT and not post SIT. Finally, although TCA and fatty acid oxidation pathway proteins were predominately differentially expressed in type I fibres following training, most of these differences were also present in the PRE samples.

Fibre-type-specific effects of different types of exercise training on mitochondrial proteins

Mitochondrial content is greater in type I compared with type II fibres (Glancy and Balaban, 2011; Leary et al., 2003) (see also Fig 2d). However, while research has reported that markers of mitochondrial content increase with exercise training (Bishop *et al.*, 2019a; Bishop et al., 2014; Larsen et al., 2012; Morgan et al., 1971), little is known about the fibre-specific effects of different types of exercise training. Consistent with our morphological (mitochondrial volume density obtained from TEM; Figures 6a & b) and biochemical (citrate synthase [CS] activity; Figure 6c) markers of mitochondrial content (Table S6-Tab 1), we observed a significant increase in the mean abundance of known mitochondrial proteins only following MICT and not SIT (Figure 6d) (Table S6-Tab 2). This can likely be attributed to the five-fold greater volume of training completed by the

MICT group (Bishop *et al.*, 2019a; Granata et al., 2018), although a consensus has yet to be reached on the relative importance of exercise intensity versus volume on training-induced changes in markers of mitochondrial content (Bishop et al., 2019b; MacInnis et al., 2019). Changes in the mean abundance of known mitochondrial proteins following MICT occurred predominantly in the type I fibres, although there was also a significant but smaller increase in the type II fibres (Figure 6d). There were no significant increases in known mitochondrial protein abundance in either fibre type following SIT (Figure 6d).

We observed fibre-type-specific adaptations of mitochondrial proteins to training, consistent with the only other single-fibre proteomic study investigating the effects of exercise training in single fibres (Deshmukh *et al.*, 2021) (Figure S1, Table S8 – Tab 1). Our results suggest that the overall mean abundance of many mitochondrial functional groups is enhanced by moderate-intensity endurance training, but only in type I fibres. As some of these proteins have been reported to decrease in aged fibres regardless of fibre type (Murgia *et al.*, 2017), it will be important to explore if other types of exercise training are able to increase the expression of these proteins in type II fibres. While changes in most mitochondrial proteins were largely confined to type I fibres following MICT, the abundance of mitochondrial ribosome proteins increased in both fibre types from PRE to POST MICT (Figure S1b, Table S8-Tab 2). These results are similar to those of another proteomic study, which revealed changes in mitochondrial ribosomal proteins in whole muscle following interval training (Robinson et al., 2017). These authors hypothesised that translational level regulation is a predominant factor controlling mitochondrial biogenesis in humans in response to exercise training. No changes in mitochondria ribosome proteins were observed in either fibre type for SIT. This suggests the volume of MICT was sufficient to induce significant mitochondrial protein synthesis in both fibre types, whereas SIT may not provide a sufficient stimulus to significantly alter mitochondrial protein synthesis (Scalzo et al., 2014).

Fibre-type-specific expression profiles for mitochondrial proteins independent of training-induced changes in mitochondrial content.

Given the greater changes in mitochondrial content that occur following MICT compared with SIT (Bishop *et al.*, 2014; Granata *et al.*, 2018; Granata et al., 2016a; Granata et al., 2016b); see also Figure 6d), we again turned our attention to investigating whether the fibre-type-specific changes in the abundance of individual mitochondrial proteins we observed with the different training types were independent of changes in total mitochondrial content. Once again, we employed our

previously described normalisation strategy to remove the bias introduced by the changes in mitochondrial content in each fibre type following both types of training (Granata *et al.*, 2021). This enabled us to investigate differences in mitochondrial protein abundances between the two fibre types without the bias introduced by training-induced changes in total mitochondrial content (Figure 7, Table S7 – Tabs 1 & 2). Post normalisation, very few training-induced changes in mitochondrial protein abundances remained in either fibre type, following either training intervention (Figure 7a). One exception was the relative decrease in the abundance of complex IV subunits in both type I and II fibres following SIT (Figure 7b & c). Thus, when changes in mitochondrial content are controlled for, very high-intensity SIT appears to deprioritise the OXPHOS components involved in the catalysis of the final step of the mitochondrial electron transport chain (i.e., complex IV). The other exception was the increase of proteins associated with fatty acid oxidation in type I fibres following MICT, which our results suggest was greater than, and not stoichiometrically linked, to the overall training-induced increase in mitochondrial content (Figure 7d). This adds to the evidence that MICT provides a powerful stimulus to increase fatty acid oxidation (Martin et al., 1993; Shaw et al., 2020); we add that this adaptation occurs predominantly in type I skeletal muscle fibres (with the exercise stimulus employed in our study).

Discussion

Proteomics applied to human skeletal muscle remains in its infancy but has introduced new opportunities to explore the complexity of the biological networks underlying fibre-specific differences and responses to exercise training. In the present study, we developed a sensitive MS-based proteomics workflow that allowed for the pooling of single muscle fibres, and the utilisation of tandem mass tag (TMT) labelling, to accommodate our complex experimental design and increase the quantitative accuracy of our results. In addition, we incorporated a much larger sample size than previous studies (i.e., 23 versus 4 to 5 participants) to better account for the individual variability in human skeletal muscle and to increase the robustness of our findings. Consistent with previous research (Deshmukh *et al.*, 2021), we identified many differentially expressed proteins between type I and type II fibres (Figure 1f). However, further analysis of these results allowed us to make two new and important observations. The first is that only 8 of the 27 mitochondrial proteins with fibre-type-specific expression profiles remained significantly different when we used our previously published normalisation strategy to account for the overall greater content of mitochondria in type I versus type II fibres (Figure 2c). Thus, many of the differences in mitochondrial protein abundances

between fibre types reported by us (Figure 2e), and others (Deshmukh *et al.*, 2021; Murgia *et al.*, 2017), are likely due to differences in total mitochondrial content rather than representing a fibre-type-specific mitochondrial proteome. The second new finding is that some of the fibre-type differences observed pre-training (especially for contraction-related proteins) were increased by moderate-intensity training. This highlights the challenge of distinguishing between protein expression profiles that are intrinsic to different fibre types and those that are a consequence of adaptations to habitual physical activity.

Repeated muscle contractions, via habitual physical activity or exercise training, provide a potent stimulus to alter the expression of proteins and confer many health benefits (Neufer *et al.*, 2015). The development of mass-spectrometry-based proteomics has revolutionised our understanding of training-induced changes in protein abundance (Egan et al., 2011; Granata *et al.*, 2021; Holloway et al., 2009; Hostrup et al., 2018), including at a fibre-specific level (Deshmukh *et al.*, 2021). However, while it is well known that adaptations depend on the characteristics of the exercise stimulus (Jamnick *et al.*, 2020), no proteomic study has investigated the effects of different exercise stimuli on fibre-type-specific adaptations. Therefore, an important feature of our study design was the use of two types of training that were very different in terms of volume, intensity, metabolic stress, and fibre recruitment patterns (Figure 3). There was a larger number of differentially expressed proteins following MICT than SIT (Figures 4 & 5), which can likely be attributed to the five-fold greater volume of training completed by the MICT group (Bishop *et al.*, 2019a; Granata *et al.*, 2018). There were also fibre-specific adaptations to both types of training, with no overlap between the changes observed in each fibre type. Most notably, increases in proteins associated with complex I of the ETC, fatty acid oxidation, the TCA cycle, and mitochondrial dynamics were mostly confined to type I fibres following MICT. This improved understanding of how mitochondrial proteins adapt to different exercise interventions may lead to more personalised exercise prescriptions to reverse some of the fibre-specific changes that occur with ageing (Murgia *et al.*, 2017) and, potentially, some chronic diseases.

Given the well-known effects of different types of training on mitochondrial content (Granata *et al.*, 2018); see also Figure 6), a further important feature of our study was to investigate whether fibre-type-specific changes in mitochondrial protein abundance were independent of training-induced changes in total mitochondrial content. To do this, we used our previously described normalisation strategy to control for the bias introduced by changes in mitochondrial content in each fibre type following both types of training (Granata *et al.*, 2021). This analysis revealed that most training-induced changes in mitochondrial protein abundances were stoichiometrically linked to the overall

increase in mitochondrial content (compare Figure 7 with Figure S1). However, a surprising observation was the decrease in the abundance of complex IV subunits, relative to the overall increase in mitochondrial protein content, in both type I and II fibres following SIT. This deprioritisation of the OXPHOS components involved in the final step of the mitochondrial electron transport chain is intriguing given that, when also controlling for changes in mitochondrial content, we have previously reported greater changes in mitochondrial respiration following SIT than MICT (Granata *et al.*, 2016a). The results of our novel normalisation strategy also revealed a discordant regulation of proteins associated with fatty acid oxidation, with a non-stoichiometric increase of these proteins in type I but not type II fibres following both types of training. Interestingly, a previous study has also reported greater increases in perilipin (PLIN) 2 and 5 in type I compared with type II fibres following both MICT and SIT (Shepherd et al., 2017). These adaptations may facilitate greater intramuscular triglyceride (IMTG) lipolysis and fatty-acid oxidation in type I fibres when metabolic demand increases (Shepherd et al., 2012; 2013).

In summary, our study incorporated several unique elements (a sensitive MS-based proteomics workflow, the largest sample size to date, two very different types of training stress, and a novel mitochondrial normalisation strategy) to identify many fibre-specific adaptations to different types of training. This provides an important resource to better understand how different fibre types adapt to different training interventions, with potential insights for how best to prescribe exercise to improve both health and human performance. In contrast to the decreased abundance of complex IV subunits in both type I and II fibres following SIT, and the increase in proteins associated with fatty acid oxidation only in type I fibres, most training-induced changes in mitochondrial protein abundances were stoichiometrically linked to the overall increase in mitochondrial content.

Limitations of the study

This study recruited healthy, young, active men and, therefore, some of the conclusions may not apply equally well to individuals of different genders, ages (e.g., the elderly), ethnicity, or health status. Another potential limitation is the use of pooled muscle fibre samples; while this assists in reducing biological variability amongst samples, it may not be a true representation of single-fibre differences both pre and post-training. Finally, it was not possible for us to determine if the fibre-specific adaptations to the two different types of exercise training had functional consequences (e.g., differences in fibre-specific mitochondrial respiratory function). It is also important to note that there

are several quantitative mass-spectrometry-based methods used to detect changes in the proteome, each with their advantages and disadvantages, and the results are not always directly comparable.

STAR METHODS

KEY RESOURCES TABLE

REAGENT or RESOURCE	SOURCE	IDENTIFIER
Antibodies		
Myosin heavy chain Type IIA	Developmental Studies Hybridoma Bank (DSHB)	A4-74 RRID: AB_528383
Anti-Myosin heavy chain Type IIB	Developmental Studies Hybridoma Bank (DSHB)	A4-840; RRID: AB_528384
Goat anti-Mouse IgG (H+L) Highly Cross-Adsorbed Secondary Antibody, Alexa Fluor Plus 488	ThermoFisher Scientific	A32723; RRID: AB_2633275
Goat anti-Mouse IgM (Heavy chain) Cross-Adsorbed Secondary Antibody, Alexa Fluor 488	ThermoFisher Scientific	A-21042; RRID: AB_2535711
Myosin heavy chain (slow, alpha- and beta-)	Developmental Studies Hybridoma Bank (DSHB)	BA-F8, RRID: AB_10572253
Myosin heavy chain (all but 2X) antibody	Developmental Studies Hybridoma Bank (DSHB)	BF-35, RRID: AB_2274680
Goat anti-Mouse IgG2b Cross-Adsorbed Secondary Antibody, Alexa Fluor 350	ThermoFisher Scientific	A-21140, RRID: AB_2535777
Goat anti-Mouse IgG1 Cross-Adsorbed Secondary Antibody, Alexa Fluor 488	ThermoFisher Scientific	A-21121, RRID: AB_2535764
Critical commercial assays		
TMT16plex Isobaric Label Reagent Set	ThermoFisher Scientific	A44521
TMTpro™ Zero Label Reagent	ThermoFisher Scientific	A44519
96-well S-Trap™ plate	Protifi	C02-96well
Deposited data		
Proteomics Reveals a Fibre-Type Specific Mitochondrial Remodelling with Moderate but not Very High Intensity Training	This paper	PRIDE: PXD036010
Software and algorithms		
ImageJ	(Schneider et al., 2012)	https://imagej.nih.gov/ij/
R version 4.1.1	R Development Core Team, 2016	https://www.R-project.org/
Proteome Discoverer 2.4	Thermofisher Scientific	
Limma 3.32.2	(Ritchie et al., 2015)	https://bioconductor.org/packages/release/bioc/html/limma.html

Resource availability

Lead contact

Further information and requests for reagent and resources may be directed to and will be fulfilled by the lead contact, Professor David J Bishop (David.Bishop@vu.edu.au).

Experimental model and Subject details

Participants and ethics approval

Twenty-eight healthy men initially volunteered to take part in this study. The data from twenty-three participants (27.2 ± 5.4 y; 178 ± 6 cm; 75.2 ± 9.7 kg; 23.6 ± 2.7 BMI; Table S1 – Tab 1) was included in the final analysis; two participants from the MICT group and two from the SIT group withdrew from the study due to time constraints, and the data from one participant was excluded from the final analysis as their muscle samples were of poor quality (see study recruitment flow chart and final group sizes; Figure S2f). Participants were provided with the information to participants' document, and were informed of the study requirements, benefits, and risks involved before giving their written informed consent. Ethics approval for the study was obtained from the Victoria University Human Research Ethics Committee (HRE17-075) and was registered as a clinical trial under Australian New Zealand Clinical Trials Registry (ANZCTR; ACTRN12617001105336).

Study design and training. During the first two weeks, participants performed two exercise familiarisation sessions and multiple testing familiarisation sessions. Participants were then allocated into one of the training groups, based on their age, body mass index (BMI), maximum rate of oxygen consumption (VO_{2max}), peak aerobic power output (W_{max}; $W \cdot kg^{-1}$), and 20-km time trial (TT) performance ($W \cdot kg^{-1}$) (all $P > 0.05$), to match the two groups for baseline endurance characteristics. The participants then underwent another week of testing and completed 8 weeks of training before the last muscle biopsy sample and final testing was performed (Figure 3a).

Sprint-Interval Training (SIT).

Twelve participants were allocated to this group (27.5 ± 5.1 y; 179 ± 6 cm; 75.5 ± 9.3 kg; 23.5 ± 2.7 BMI). The SIT group completed 4 to 8 30-second "all-out" cycling sprints against a resistance set at 0.075 kg/kg body mass (BM), interspersed with a 4-min recovery period between sprints (Gillen et al., 2016; Granata *et al.*, 2016a). The training load was increased to 0.080 $kg \cdot kg^{-1}$ BM in week 3, to 0.085 $kg \cdot kg^{-1}$ BM in week 5, and to 0.090 $kg \cdot kg^{-1}$ BM in week 7. During the recovery, participants remained on the bikes and were allowed to either rest or cycle against no resistance. Participants started the training with 4 sprints per session and this increased up to 8 sprints per session in week 7.

Moderate-Intensity Continuous Training (MICT).

Twelve participants were allocated to this group (26.9 ± 5.6 y; 178 ± 6 cm; 74.9 ± 10.2 kg; 23.7 ± 2.6 BMI). The training intensity for the MICT training group was established as 10% less than the

first lactate threshold (~ 90% of the lactate threshold 1 (LT1; defined as the first increase of ≥ 0.3 $mmol \cdot L^{-1}$ of lactate from the previous stage during the submaximal test) for 60-120 min, 3-4/wk over 8 wk) consisting of continuous cycling at a fixed power. The training intensity prescription was reassessed during the first training session of week 3, 5, and 7 and modified accordingly. At the commencement of training participants began training for 60 min per session and this increased up to 120 min per session in week 7.

Testing procedures. Participants were required to avoid any vigorous exercise for the 48 h preceding each performance test (72 h for the skeletal muscle biopsy), and to avoid caffeine consumption for at least 8 h prior to each test. Tests were performed at a similar time of the day throughout the study to avoid variations caused by changes in circadian rhythm.

GXT. Graded exercise tests (GXTs) were performed on an electronically-braked cycle ergometer (Lode Excalibur v2.0, Groningen, The Netherlands) to determine maximal oxygen uptake ($V\square O_{2max}$) and maximal aerobic power ($W\square_{max}$). A GXT design of 1-min incremental stages was utilised, aiming to attain a total testing duration of 9 to 11 minutes. Breath-by-breath recordings of $V\square O_2$, $V\square CO_2$, and $V\square_E$ were acquired throughout the GXT using a metabolic analyser (Quark Cardiopulmonary Exercise Testing, Cosmed, Italy). Upon exhaustion, a 5-min recovery was given to participants, and a verification exhaustive bout was performed at an intensity equivalent to 90% of $W\square_{max}$ to confirm the highest measured $V\square O_{2max}$ (Jamnick et al., 2018). The $W\square_{max}$ was determined as the average power of the last minute completed.

Submaximal test. Once the initial GXT was completed, the ventilatory parameters obtained ($V\square O_2$, $V\square CO_2$, $V\square_E$) were used to estimate VT1. Once estimated, the submaximal test started at 40 W lower than the estimated VT1 and the intensity was increased 10 W every 3 min (stage length) until the LT1 was surpassed and identified. The test was stopped at a blood lactate of 2 $mmol \cdot L^{-1}$ as the LT1 had been reached in all cases. Antecubital venous blood was taken in the last 15 s of each stage and was instantly analysed in duplicate using a blood lactate analyser (YSI 2300 STAT Plus, YSI, USA).

Physical activity and nutritional controls. Participants were requested to maintain a normal dietary pattern and physical activity throughout the study. To minimise the variability in muscle metabolism, participants were provided with a standardised dinner (55 kJ/kg of body mass (BM), providing 2.1 g carbohydrate/kg BM, 0.3 fat/kg BM, and 0.6 g protein/kg BM) and breakfast (41 kJ/kg BM,

providing 1.8 g carbohydrate/kg BM, 0.2 g fat/kg BM, and 0.3 g protein/kg BM) to be consumed 15 h and 3 h before the biopsies, respectively.

Muscle biopsies and single muscle fibre isolation. A biopsy needle with suction was used to obtain vastus lateralis muscle biopsies under local anaesthesia (1% xylocaine) at pre training and three days post training. After being cleaned of excess blood, connective tissue, and fat, muscle biopsies were divided as follows: one piece of muscle was placed in RNALater® (R0901, Sigma Aldrich, Australia) on the biopsy day and stored at 4 °C, and then separated on ice into single fibres within a few days. Forty fibres from each biopsy were individually isolated, and cut into half, with one half of the fibre stored in RNA*Later*™ (R0901, Sigma Aldrich, Australia)) and the remaining fibre halves were placed in a Laemmli solution (a solubilising buffer) (Murphy, 2011). The Laemmli solution was composed of 4% (v/v) sodium dodecyl sulfate (SDS), a thiol agent of 10% (v/v) ß-mercaptoethanol, 20% (v/v) glycerol, 0.125 M tris-hydroxymethyl-aminomethane (tris)-HCl; and 0.015 % (v/v) bromophenol blue, pH 6.8. Each fibre was diluted with 5 µL of 3x the solubilising buffer 2:1 (v/v) with 10 µL of 1x Tris-Cl (pH 6.8) (Murphy, 2011; Wyckelsma *et al.*, 2015). These fibre segments were then immediately frozen in liquid nitrogen and stored at ¯80 ºC.

Single Muscle Fibre Analysis – Immunoblotting

Muscle Fibre Typing (Dot Blotting)

To assess muscle fibre types, PVDF membranes were activated in 95% ethanol for 15 to 60 s and then equilibrated for 2 min in transfer buffer (25 mM Tris, 192 mM glycine, pH 8.3 and 20% methanol). The wet membrane was then placed on a stack of filter paper (one to two pieces soaked in transfer buffer on top of one dry piece). The single fibre samples in the Laemmli solution were then thawed and vortexed, but not centrifuged to avoid pelleting and hence loss of any of the skeletal muscle protein (Murphy, 2011). Samples were spotted to a specific part of the membrane in aliquots equating to ~ 1/8 of a fibre segment (i.e., 1 µL) using a multi-channel pipette. This was repeated twice, once for type I fibre detection and another time for type II fibre detection. After complete absorption of samples, the membrane was placed on top of a dry piece of filter paper to dry for 2 to 5 min before being reactivated in 95% ethanol for 15 to 60 s and equilibrated in transfer buffer for 2 min. After three quick washes in Tris-buffered saline-Tween (TBST), the membrane was blocked in 5% non-fat milk in TBST (blocking buffer) for 5 min at room temperature. Following blocking, the membrane was rinsed with TBST and then incubated in MHCIIa (#A4.74, Developmental Studies

Hybridoma Bank [DSHB]) or MHCI (#A4.840, DSHB) antibody overnight at 4 ºC with gentle rocking. On the second day, membranes were washed in TBST and then incubated in secondary antibody IgG (MHCIIa, #A32723, ThermoFisher Scientific) or IgM (MHCI, # Cat # A-21042 4, ThermoFisher Scientific) at room temperature for 1 h with rocking. Lastly, membranes were washed in TBST and then exposed to Clarity enhanced chemiluminescence reagent (BioRad, Hercules, CA, USA), imaged (ChemiDoc MP, BioRad), and analysed for signal density (ImageLab 5.2.1, BioRad) (See example image in Figure 1a). Using images of all the membranes, it was possible to determine the fibre type of each sample (I or IIa) or if no MHC protein was present (Christiansen et al., 2019), which would indicate unsuccessful collection of a fibre segment. Samples with signal density in both type I and IIa membranes were discarded (i.e., I/IIa hybrid, two different fibres in the same sample).

Muscle glycogen fibre-type histochemistry analysis

Muscles were embedded in O.C.T. compound (Tissue-Tek), frozen in liquid nitrogen-cooled isopentane, stored at ¯80 °C, and cut into 10 µm thick cryosections with a cryostat (Leica) maintained at −20 °C.

Fibre type-specific glycogen depletion was imaged under brightfield using periodic acid-Schiff stain (PAS), similar to the methodology described elsewhere (Schaart et al., 2004). As such, 10 µm thick muscle cryosections were serially sectioned onto cleaned glass slides and subsequently fixed in 3.7% formaldehyde in 90% ethanol for 60 min at 4˚C. After this fixation, sections were then pre-treated for 5 min with 1% periodic acid (Sigma-Aldrich, Australia) in milliQ-water followed by a washing step for 1 min in tap water and a wash dip for 5 s in milliQ-water. The slides were then applied with 15% diluted Schiff's reagent in PBS (Sigma-Aldrich, Australia) and incubated for 15 min at room temperature. The Schiff's reagent was diluted to 15% based on prior optimisation, as when applied without any dilution the dye intensity saturated the signal. After Schiff's reagent, the sections were washed for 5 s in milliQ-water followed by a 10-min rinse with tap water. Thereafter, sections were washed (3 x 5 min) in PBS (137 $mmol.L^{-1}$ sodium chloride, 3 $mmol.L^{-1}$ potassium chloride, 8 $mmol.L^{-1}$ sodium phosphate dibasic and 3 $mmol.L^{-1}$ potassium phosphate monobasic, pH of 7.4). Slides were then dried before adding ~ 15 µL of PBS per section and mounting with cover slips. The slides were then viewed and imaged in high resolution using an Olympus BX51 fluorescence microscope (Olympus Corporation, Tokyo, Japan) and Cell F software (Olympus). All images were obtained with the x10 objective and captured under bright-field mode.

The second serially sectioned slide underwent immunofluorescence staining of MHC expression performed with 1:25 primary antibodies against MHCI (BA-F8) and MHCIIa (BF-35) (Developmental Studies Hybridoma Bank, University of Iowa), whereas secondary antibodies were Alexa fluor 350 IgG_{2b} 1:500 (blue) and Alexa fluor 488 IgG_{2b} 1:500 (green) (Invitrogen). Antibody cocktail configurations and immunofluorescence staining procedures were followed according to Bloemberg et al. (Bloemberg and Quadrilatero, 2012). Once completely dry, the sections were incubated (blocked) with 10% goat serum (product no: 50197Z, ThermoFisher Scientific) for one hour. The excess goat serum was then removed, and sections were incubated with primary fibre type antibodies over night at 4 ºC. The following morning, the primary antibodies were washed off in milliQ water (3 x 5 minutes). Once the slides were fully dry, they were incubated with fluoro-conjugated secondary antibodies for 90 minutes. Slides were washed further with milliQ water (3 x 5 minutes) post incubation and dried before adding ~ 15 µL of PBS per section and mounting with cover slips. The slides were then viewed and imaged in high resolution using an Olympus BX51 fluorescence microscope (Olympus Corporation, Tokyo, Japan) and Cell F software (Olympus). All images were obtained with the x10 objective and analysis of images was performed using Image J software (National Institutes of Health, Maryland, USA) (See Figure 3a for example images).

Citrate Synthase (CS) Activity Assay.

CS activity was performed on a 96-well plate by combining 5 µL of a 2 $\mu g \cdot \mu L^{-1}$ muscle lysate, 40 µL of 3 mM acetyl CoA, and 25 µL of 1 mM DTNB to 165 µL of 100 mM Tris buffer (pH 8.3). Following 15 µL of 10 mM oxaloacetic acid was added to the plate mixture, protected from the light, and immediately placed in the spectrophotometer at 30 °C (xMark Microplate Spectrophotometer, Bio-Rad Laboratories Pty Ltd, Gladesville, NSW, AUS). Absorbance was recorded at 412 nm every 15 s for 6 min after 30 s of mixture agitation. CS activity was calculated from the steepest part of the curve and reported as $mol \cdot kg\ protein^{-1} \cdot h^{-1}$.

Blood Lactate and pH measurements

Antecubital venous blood samples (~ 1 mL) were collected pre and post the first exercise training session from a cannula inserted in the antecubital vein for the determination of venous blood $[H^+]$ and lactate concentrations using a blood-gas analyser (ABL 800 FLEX, Radiometer Copenhagen).

Transmission Electron Microscopy.

Skeletal muscle samples were fixed overnight at 4 °C with 0.2 M sodium cacodylate– buffered, 2.5% glutaraldehyde, and 2% paraformaldehyde. Fixed samples were rinsed with 0.1 M sodium cacodylate, and postfixed with ferricyanide-reduced osmium tetroxide (1% OsO4, 1.5% K3 [Fe(CN)6], and 0.065 M cacodylate buffer) for 2 h at 4°C. The postfixed samples, were processed by the Monash Ramaciotti Centre for Cryo-Electron Microscopy, were rinsed with distilled water and then stored overnight in 70% ethanol. Dehydration was performed by graduated ethanol series (80%, 90%, 95%, 100%, and 100%; 10 min each) and propylene oxide (100% and 100%; 5 min each). Samples were infiltrated with Araldite 502/Embed 812 by graduated concentration series in propylene oxide (25% for 1 h, 33% for 1 h, 50% overnight; 66% for 4 h, 75% for 4 h, 100% overnight; and 100% for 5 h) and then polymerised at 60 °C for 48 h. Embedded samples were sectioned using an Ultracut UCT ultramicrotome (Leica Biosystems) equipped with a 45° diamond knife (Diatome) to cut 75-nm ultrathin sections. The grids were stained at room temperature using 2% aqueous uranyl acetate (5 min) and Reynolds lead citrate (3 min) before routine imaging. All TEM imaging was performed at 80 kV on a Jeol JEM-1400Plus and recorded with a Matataki flash camera and DigitalMicrograph (Version 1.71.38) acquisition software.

Proteome Sample preparation

Fibres were placed into 5 µL of 2x SDS solubilising buffer (0.125 M Tris·Cl, pH 6.8, 4% SDS, 10% glycerol, 4 M urea, 5% mercaptoethanol, 0.001% bromophenol blue) diluted 2 times (vol/vol) with 1 x Tris·Cl, pH 6.8. Fibres were pooled according to fibre type and further lysed with heating at 95 °C for 10 min. The pooled fibres were then sonicated for 20 min (Bioruptor, Diagenode, 20 cycles of 30 s). Reduction and alkylation of disulfides was performed by adding chloroacetamide (40 mM, CAA, Sigma) and further incubated for 30 min at 50 °C. The SDS lysate was acidified with 12% aqueous phosphoric acid at 1:10 for a final concentration of ~ 1.2% phosphoric acid and mixed. This step was essential as the proteins are filtered at this pH. The high percentage of methanol can then precipitate the protein out, which will be retained on top of the S-Trap™ (ProtiFi). Following this, 350 µL of S-Trap™ buffer (90% Methanol (MeOH) and 100 mM triethylammounium bicarbonate (TEAB), $C_7H_{17}NO_3$) was added to the acidified lysis buffer (final pH 7.1). A colloidal protein particulate was instantly formed in this step. With the S-Trap™ micro column in a 1.7 mL tube for flow through, the acidified SDS lysate/MeOH S-Trap™ buffer mixture was added into the micro column. The micro column was then centrifuged at 6500 rpm for 30 s until all SDS lysate/ S-Trap™ buffer had passed through the S-Trap™ column. Protein was then trapped within the protein-trapping matrix of the spin

column. The captured protein was then washed with 350 µL S-Trap™ buffer with centrifugation and washing repeated three times. The spin column was then transferred to a fresh 1.7 mL tube (this aided in preventing contamination of the digestion). For best results, the S-Trap™ micro column was rotated 180 degrees between the centrifugation washes. The S-Trap™ micro column was then moved to a clean 1.7 mL sample tube for the digestion with the protease (trypsin and LysC added at a concentration of 1:50 in 125 µL of 50 mM digestion buffer) into the top of the micro column. The sample was then centrifuged at a low speed of 1000 rpm for 30 s and any solution that passes through is returned to the top of the column (the protein-trapping matrix is highly hydrophilic and will absorb the solution; however, it was important to ensure there was no bubble at the top of the protein trap). The column was then transferred to another fresh tube and incubated at 37 °C overnight (~ 16 hours). For 96-well plates, the protease combination was added at a concentration of 1:25 in 125 µL of 50 mM digestion buffer and incubated for 1 hour at 47 °C.

Peptides were eluted with 80 µL each of digestion buffer (50 mM TEAB) and then 0.2% aqueous formic acid was added to the S-Trap™ protein trapping matrix centrifuged at 3600 rpm for 60 s for each elution. Hydrophobic peptides were recovered with an elution of 80 µL 60% (v/v) acetonitrile containing 0.2% formic acid and then centrifuged at 6500 rpm for 60 s. Elutions were pooled.

Further peptide purification was performed as required with 2x SDB-RPS disc stage tips that were prepared and had sample loaded onto the stage-tip. Peptides were then centrifuged through the column at 1500 g for 3 min. Stage tips were washed with 100 uL of 90% isopropanol (C_3H_8O) containing 1% TFA and then washed again with 0.2% TFA in 5% acetonitrile and centrifuged for 4 min following each wash. Peptides were then eluted by adding 100 uL of 60% acetonitrile containing 5% ammonium hydroxide and centrifuged for 4 min. Samples were lyophilised down to dryness with the SpeedVac (CentriVap Benchtop Centrifugal Vacuum Concentrator, # 7810038, VWR) and reconstituted for labelling and subsequent MS analysis.

TMTpro Labelling

TMTpro Label Reagents (ThermoFisher) were equilibrated to room temperature and 20 µL of anhydrous acetonitrile was added to each tube. Dried samples were reconstituted in 0.5 M HEPES buffer, pH 8.5. The desired amount of TMTpro label was added and incubated at 20 °C for 1 h with shaking (1000 rpm). The reaction was then quenched by adding a final concentration of 0.25% of hydroxylamine to the peptide and TMT mixture, and further incubated at 20 °C for 30 min. Samples

were lyophilised down to dryness with the SpeedVac and reconstituted in loading buffer. Each sample was fractionated into 16 fractions using basic pH reverse phase C18 liquid chromatography. Peptides were subjected to basic-pH reverse-phase high pressure liquid chromatography (HPLC) fractionation. Labelled peptides were solubilised in buffer A (10 mM ammonium hydroxide) and separated on an Agilent HpH Poroshell120 C18 column (2.7 μm particles, 2.1 mm i.d., and 5 cm in length).

TMT Labelling Strategy

Multiplexing techniques have recently extended from 11 to 16 plex, which not only increases sample throughput but accommodates complex experimental designs such as this training study. This provided the ability to label 16 samples in one go and then merge as one sample through the LC-MS. A 16-plex also allows for an expanded number of treatments, such as replicates, and dose-response or time-course measurements can be analysed in the same experiment with basically no missing values across all samples and extending the statistical power across the entire system (Li et al., 2020). The main study used TMTpro 16-plex version with a different reporter and mass normaliser than earlier TMT versions (i.e., TMT-6 plex). A limitation of tag-based proteomic strategies is ion interference-related ratio distortion resulting from fragmentation and analysis of background ions co-isolated with those of interest. Each sample is differentially labelled, such that when pooled the signal-to-noise values of sample-specific reporter ions represent the relative abundance of each protein. As such, the degree of ion interference by the level of TMT signal detected in channels where a specific protein should be absent can be assessed (Brenes et al., 2019). To best accommodate for possible reporter ion interferences, we followed a sampling strategy that is illustrated in Figure S2g. Reporter ion interference (RII) targets were classified according to a typical product data sheet for 16-plex TMTpro Label Reagents from ThermoFisher Scientific.

Liquid Chromatography-MS/MS Acquisition

Peptides were loaded onto a 2-cm PepMap trap column (ThermoFisher) and separated using a PepMap 75 μm × 50 cm column (ThermoFisher) with a gradient of 2–30% MeCN containing 0.1% FA over 120 min at 250 nL/min and at 40 °C. The Orbitrap Fusion mass spectrometer was operated with the following parameters: an MS1 scan was acquired from 375–1575 m/z (120,000 resolution, 2e5 AGC, 50 ms injection time) followed by MS2 data-dependent acquisition with collision-induced dissociation (CID) and detection in the ion trap (4e3 AGC, 150 ms injection time, 30 NCE, 1.6 m/z quadrupole isolation width, 0.25 activation Q). To quantify TMTpro reporter ions, a synchronous precursor selection MS3 scan was performed with higher-energy collisional dissociation (HCD) and

detection in the orbitrap (120 to 750 m/z, 1e5 AGC, 250 ms injection time, 60 NCE, 2.5 m/z isolation width). The total cycle time was set to 2.5 s. The acquired raw data was analysed with Proteome Discoverer 2.4 (ThermoFisher) and the non-normalised protein reporter intensity was exported to Excel and further analysed in R.

Bioinformatic analysis of proteomics data.

Clean up and normalisation

Only proteins that had a high FDR confidence, were not deemed a contaminant, and had greater than one unique peptide, were used for analysis. Proteins having < 70% valid values were removed and the remaining missing data was imputed using k nearest neighbour (knn) method from the *impute* package in R. Normalisation was performed using a combination of trimmed mean of M values (TMM), sample loading (SL), and ComBat (v0.0.4) methods (Johnson et al., 2007; Liu et al., 2004; Plubell et al., 2017; Robinson and Oshlack, 2010). Sample loading adjusts each TMT experiment to an equal signal per channel and TMM uses the average or median signal that is typically applied to use a single multiplicative factor to further adjust the samples to each other. Further to this, ComBat allows users to adjust for batch effects in datasets where the batch covariate is known, using previously described methodology (Johnson *et al.*, 2007).

Differential expression analysis

Differential expression analysis was performed using the R package *limma* (v3.48.3) (Ritchie *et al.*, 2015) on the relative protein abundances after first performing the normalisation technique described above. Differential expression values were determined by comparing the expression. To focus on proteins specifically associated with fibre type, the differential expression comparisons were first filtered to include proteins differentially expressed between type I and type II fibres before exercise (adjusted P value < 0.05). This established the baseline of the proteins that were significantly different between the two fibre types prior to exercise and allowed for comparisons between our data and the data of Murgia et. al. (2017) and Deshmukh et. al. (2020) (Figures 1 and 2). Following this, comparisons were made to identify any significant effects (Fusion Factor P value < 0.05) exercise produced on each of the fibre types for each type of exercise (MICT type I Pre vs Post, MICT type II Pre vs Post, SIT type I Pre vs Post, SIT type II Pre vs Post; Figure 4). Finally, comparisons were completed between fibre types on samples post exercise (MICT Post type I vs type II and SIT Post type I vs type II, Figure 4), to distinguish and compare significant (adjusted P value < 0.05) differences between the fibre types after exercise. Mitochondrial proteins were identified by

annotation using both the Integrated Mitochondrial Protein Index (IMPI) and the Mitocarta 3.0 database (Rath et al., 2020).

The heatmap presented in Figure 1g was completed using the *ComplexHeatmap* package (v.2.8.0), with hierarchical clustering using the "average" method. The heatmap presented in Figure 7c was created using the native R heatmap function and clustered according to the OXPHOS complex subunits as identified in MitoCarta 3.0. For visualisations of differential expression comparisons, volcano plots were presented in Figure 1f, 2,e,f, 5a,b and used the resulting adjusted P values from the *limma* analysis, which can be found in Table S1, S2, S3 and S4. Volcanos from Figure 4 a,b used the P values from the Fusion Factor calculation found in Table S4. Profile Plots presented in Figures 6d, 7a,b,d and S1b,c, were created by calculating a mean of the group in question (complex or functional group as identified by MitoCarta 3.0) with all proteins identified in that group coloured and a background displayed of all mitochondrial proteins (with an exception for Figure 7a, which used all proteins identified). Statistical significance between Pre and Post training values within the profile plots was completed using a paired t-test and the default adjustment for multiple hypothesis testing. Venn diagrams featured in Figure 1c, 2a were created using the *VennDiagram* (v1.7.1) package.

To better characterise the proteomic changes, gene ontology and enrichment analysis were performed by investigating non-random associations between proteins and over-represented Gene Ontology (GO). For Figures 1b, we calculated the average number of proteins in each pooled sample, the proteins identified within the entire dataset of high confidence proteins and compared them to the entire human genome to determine how many were identified in specific GO CC terms compared to the human genome. Figure 1d and 2b compared the 846 and 272 proteins respectively, which were common between the three datasets investigated and the top five GO CC terms for the 846 proteins were visualised, with the top five GO BP terms used for the 273. These analyses were conducted using Database for Annotation, Visualization and Integrated Discovery (DAVID) (Huang et al., 2009). Network plots and WikiPathways are presented in Figure 5e and f respectively. The network plot (Figure 5f) was completed using only statistically significant (adjusted P value < 0.05) results for the comparisons of type I vs II values post both MICT and SIT, whereas the Wikipathways BubblePlot uses all results for the same comparisons. These analyses were completed using the R package *ClusterProfiler* (v4.0.5).

Mitochondrial Normalisation

As the mitochondrial protein expression identified a difference in the mitochondrial content between the two fibre types before exercise, we employed a previously reported normalisation strategy (Granata *et al*., 2021). This normalisation strategy removes bias introduced by the differences in mitochondrial content and allows the investigation of these adaptations when this bias was removed. Mitochondrial proteins identified through IMPI and MitoCarta 3.0 were subset from the rest of the data, and the same normalisation protocol as reported above was applied.

Data availability and code availability

- Source data to interpret, verify, and extend this research is provided with this paper. The mass spectrometry proteomics data has been deposited in the ProteomeXchange Consortium via the PRIDE partner repository under accession code PXD036010.

- The R scripts used for all omics analyses described above are deposited on GitHub and available through https://doi.org/10.5281/zenodo.7227801. There are no restrictions placed on accessibility of this code.

Author Contributions Statement

D.J.B., J.B, E.R., and C.G. conceptualised and designed the study. J.B. carried out the training study and sample collection. E.R., J.B., and C.H. performed the experiments. E.R and S.C. performed muscle glycogen fibre-type histochemistry analysis. V.O and G.R. performed the electron microscopy experiments. N. J. C. performed the statistical and bioinformatic analysis. D.J.B., E.R., and N.J.C. wrote the manuscript. E.R., J.B., C.H, R.B.S. D.A.S, C.G., N.J.C and D.J.B. edited and revised the manuscript. All persons designated as authors qualify for authorship, and all those qualifying for authorship are listed. All authors have read and approved the final manuscript.

Acknowledgments

We thank Iresha Hanchapola from Monash Proteomics & Metabolomics Facility for proteomic supplies and instrument support and acknowledge Associate Professor Javier Diaz Lara from the University de Navarra for support with dot blotting.

Funding

This study was supported by grants from the Australian Research Council (Discovery Projects DP140104165 and DP160102176 to D.J.B) the Australian Physiological Society (Ph.D. grant to J.B), and the Australian National Health and Medical Research Council (NHMRC Fellowship GNT2009732 to D.A.S.). J.B. was supported by a Victoria University International Postgraduate Research Scholarship.

Competing Interests Statement

The authors declare no conflict of interest.

References

Bergh, U., Thorstensson, A., Sjödin, B., Hulten, B., Piehl, K., and Karlsson, J. (1978). Maximal oxygen uptake and muscle fiber types in trained and untrained humans. Med Sci Sports *10*, 151-154.

Bishop, D.J., Botella, J., Genders, A.J., Lee, M.J., Saner, N.J., Kuang, J., Yan, X., and Granata, C. (2019a). High-Intensity Exercise and Mitochondrial Biogenesis: Current Controversies and Future Research Directions. Physiology (Bethesda, Md.) *34*, 56-70. 10.1152/physiol.00038.2018.

Bishop, D.J., Botella, J., and Granata, C. (2019b). CrossTalk opposing view: Exercise training volume is more important than training intensity to promote increases in mitochondrial content. The Journal of Physiology *0*. 10.1113/JP277634.

Bishop, D.J., Granata, C., and Eynon , N. (2014). Can we optimise the exercise training prescription to maximise improvements in mitochondria function and content? . Biochimica et Biophysica Acta *1840*, 1266–1275.

Bloemberg, D., and Quadrilatero, J. (2012). Rapid Determination of Myosin Heavy Chain Expression in Rat, Mouse, and Human Skeletal Muscle Using Multicolor Immunofluorescence Analysis. PLOS ONE *7*, e35273. 10.1371/journal.pone.0035273.

Brenes, A., Hukelmann, J., Bensaddek, D., and Lamond, A.I. (2019). Multibatch TMT Reveals False Positives, Batch Effects and Missing Values. Mol Cell Proteomics *18*, 1967-1980. 10.1074/mcp.RA119.001472.

Christiansen, D., MacInnis, M.J., Zacharewicz, E., Xu, H., Frankish, B.P., and Murphy, R.M. (2019). A fast, reliable and sample-sparing method to identify fibre types of single muscle fibres. Scientific Reports *9*, 6473. 10.1038/s41598-019-42168-z.

Deshmukh, A.S., Murgia, M., Nagaraj, N., Treebak, J.T., Cox, J., and Mann, M. (2015). Deep Proteomics of Mouse Skeletal Muscle Enables Quantitation of Protein Isoforms, Metabolic Pathways, and Transcription Factors Molecular and Cell Proteomics *14*, 841-853.

Deshmukh, A.S., Steenberg, D.E., Hostrup, M., Birk, J.B., Larsen, J.K., Santos, A., Kjøbsted, R., Hingst, J.R., Schéele, C.C., Murgia, M., et al. (2021). Deep muscle-proteomic analysis of freeze-dried human muscle biopsies reveals fiber type-specific adaptations to exercise training. Nature Communications *12*, 304. 10.1038/s41467-020-20556-8.

Dudley, G.A., Abraham, W.M., and Terjung, R.L. (1982). Influence of exercise intensity and duration on biochemical adaptations in skeletal muscle. Journal of applied physiology: respiratory, environmental and exercise physiology *53*, 844-850. 10.1152/jappl.1982.53.4.844.

Egan, B., Dowling, P., O'Connor, P.L., Henry, M., Meleady, P., Zierath, J.R., and O'Gorman, D.J. (2011). 2-D DIGE analysis of the mitochondrial proteome from human skeletal muscle reveals time coursedependent remodelling in response to 14 consecutive days of endurance exercise training Proteomics *11*, 1413–1428.

Egan, B., and Zierath, J.R. (2013). Exercise metabolism and the molecular regulation of skeletal muscle adaptation. Cell Metab. *17*, 162-184. 10.1016/j.cmet.2012.12.012.

Galpin, A.J., Raue, U., Jemiolo, B., Trappe, T.A., Harber, M.P., Minchev, K., and Trappe, S. (2012). Human skeletal muscle fiber type specific protein content. Analytical biochemistry *425*, 175-182. 10.1016/j.ab.2012.03.018.

Gillen, J.B., Martin, B.J., MacInnis, M.J., Skelly, L.E., Tarnopolsky, M.A., and Gibala, M.J. (2016). Twelve Weeks of Sprint Interval Training Improves Indices of Cardiometabolic Health Similar to Traditional Endurance Training despite a Five-Fold Lower Exercise Volume and Time Commitment. PLoS One *11*, e0154075. 10.1371/journal.pone.0154075.

Glancy, B., and Balaban, R.S. (2011). Protein composition and function of red and white skeletal muscle mitochondria. American journal of physiology. Cell physiology *300*, C1280-C1290. 10.1152/ajpcell.00496.2010.

Godin, R., Ascah, A., and Daussin, F.N. (2010). Intensity-dependent activation of intracellular signalling pathways in skeletal muscle: role of fibre type recruitment during exercise. J Physiol *588*, 4073-4074. 10.1113/jphysiol.2010.195925.

Gollnick, P.D., Piehl, K., and Saltin, B. (1974). Selective glycogen depletion pattern in human muscle fibres after exercise of varying intensity and at varying pedalling rates. J Physiol *241*, 45-57. 10.1113/jphysiol.1974.sp010639.

Granata, C., Caruana, N.J., Botella, J., Jamnick, N.A., Huynh, K., Kuang, J., Janssen, H.A., Reljic, B., Mellett, N.A., Laskowski, A., et al. (2021). High-intensity training induces non-stoichiometric changes in the mitochondrial proteome of human skeletal muscle without reorganisation of respiratory chain content. Nature Communications *12*, 7056. 10.1038/s41467-021-27153-3.

Granata, C., Jamnick, N.J., and Bishop, D.J. (2018). Training-induced mitochondrial adaptations. Sports Med., 1-20.

Granata, C., Oliveira, R.S., Little, J.P., Renner, K., and Bishop, D.J. (2016a). Training intensity modulates changes in PGC-1α and p53 protein content and mitochondrial respiration, but not markers of mitochondrial content in human skeletal muscle. Faseb j *30*, 959-970. 10.1096/fj.15-276907.

Granata, C., Oliveira, R.S.F., Little, J.P., Renner, K., and Bishop, D.J. (2016b). Mitochondrial adaptations to high-volume exercise training are rapidly reversed after a reduction in training volume in human skeletal muscle The Federation of American Societies for Experimental Biology Journal *30*, 1-11.

Greenhaff, P.L., Nevill, M.E., Soderlund, K., Bodin, K., Boobis, L.H., Williams, C., and Hultman, E. (1994). The metabolic responses of human type I and II muscle fibres during maximal treadmill sprinting. The Journal of Physiology *478*, 149-155. https://doi.org/10.1113/jphysiol.1994.sp020238.

Hargreaves, M., and Spriet, L.L. (2020). Skeletal muscle energy metabolism during exercise. Nature Metabolism *2*, 817-828. 10.1038/s42255-020-0251-4.

Hawley, J.A., Hargreaves, M., Joyner, M.J., and Zierath, J.R. (2014). Integrative biology of exercise. Cell *159*, 738-749. 10.1016/j.cell.2014.10.029.

Henneman, E. (1957). Relation between Size of Neurons and Their Susceptibility to Discharge. Science (New York, N.Y.) *126*, 1345. 10.1126/science.126.3287.1345.

Henneman, E., and Olson, C.B. (1965). Relations Between Structure and Function in the Design of Skeletal Muscle. Journal of Neurophysiology *28*, 581-598. 10.1152/jn.1965.28.3.581.

Holloszy, J.O., and Coyle, E.F. (1984). Adaptations of skeletal muscle to endurance exercise and their metabolic consequences. Journal of applied physiology: respiratory, environmental and exercise physiology *56*, 831-838. 10.1152/jappl.1984.56.4.831.

Holloway, K.V., O'Gorman, M., Woods, P., Morton, J.P., Evans, L., Cable, N.T., Goldspink, D.F., and Burniston, J.G. (2009). Proteomic investigation of changes in human vastus lateralis muscle in response to interval-exercise training. Proteomics *9*, 5155-5174. 10.1002/pmic.200900068.

Hostrup, M., Onslev, J., Jacobson, G.A., Wilson, R., and Bangsbo, J. (2018). Chronic β2-adrenoceptor agonist treatment alters muscle proteome and functional adaptations induced by high intensity training in young men. The Journal of Physiology *596*, 231-252. 10.1113/JP274970.

Howald, H., Hoppeler, H., Claassen, H., Mathieu, O., and Straub, R. (1985). Influences of endurance training on the ultrastructural composition of the different muscle fiber types in humans. Pflugers Archiv : European journal of physiology *403*, 369-376. 10.1007/bf00589248.

Huang, D.W., Sherman, B.T., and Lempicki, R.A. (2009). Systematic and integrative analysis of large gene lists using DAVID bioinformatics resources. Nature protocols *4*, 44-57. 10.1038/nprot.2008.211.

Ingjer, F. (1979). Effects of endurance training on muscle fibre ATP-ase activity, capillary supply and mitochondrial content in man. The Journal of Physiology *294*, 419-432. 10.1113/jphysiol.1979.sp012938.

Jackman, M.R., and Willis, W.T. (1996). Characteristics of mitochondria isolated from type I and type IIb skeletal muscle. American Journal of Physiology-Cell Physiology *270*, C673-C678. 10.1152/ajpcell.1996.270.2.C673.

Jamnick, N.A., Botella, J., Pyne, D.B., and Bishop, D.J. (2018). Manipulating graded exercise test variables affects the validity of the lactate threshold and V˙ O2peak. PLoS One *13*, e0199794.

Jamnick, N.A., Pettitt, R.W., Granata, C., Pyne, D.B., and Bishop, D.J. (2020). An Examination and Critique of Current Methods to Determine Exercise Intensity. Sports Medicine. 10.1007/s40279-020-01322-8.

Jansson, E., Sjodin, B., and Tesch, P. (1978). Changes in muscle fibre type distribution in man after physical training. A sign of fibre type transformation? Acta Physiol Scand *104*, 235-237. 10.1111/j.1748-1716.1978.tb06272.x.

Johnson, W.E., Li, C., and Rabinovic, A. (2007). Adjusting batch effects in microarray expression data using empirical Bayes methods. Biostatistics *8*, 118-127. 10.1093/biostatistics/kxj037.

Kiessling, K.H., Piehl, K., and Lundquist, C.G. (1971). Effect of Physical Training on Ultrastructural Features in Human Skeletal Muscle. In Muscle Metabolism During Exercise: Proceedings of a Karolinska Institutet Symposium held in Stockholm, Sweden, September 6–9, 1970 Honorary guest: E Hohwü Christensen, B. Pernow, and B. Saltin, eds. (Springer US), pp. 97-101. 10.1007/978-1-4613-4609-8_9.

Kiessling, K.H., Pilström, L., Bylund, A.C., Saltin, B., and Piehl, K. (1974). Enzyme Activities and Morphometry in Skeletal Muscle of Middle-Aged Men after Training. Scandinavian journal of clinical and laboratory investigation *33*, 63-69. 10.3109/00365517409114199.

Kristensen, D.E., Albers, P.H., Prats, C., Baba, O., Birk, J.B., and Wojtaszewski, J.F. (2015). Human muscle fibre type-specific regulation of AMPK and downstream targets by exercise. J Physiol *593*, 2053-2069. 10.1113/jphysiol.2014.283267.

Lamboley, C.R., Wyckelsma, V.L., Dutka, T.L., McKenna, M.J., Murphy, R.M., and Lamb, G.D. (2015). Contractile properties and sarcoplasmic reticulum calcium content in type I and type II skeletal muscle fibres in active aged humans. J Physiol *593*, 2499-2514. 10.1113/jp270179.

Larsen, S., Nielsen, J., Hansen, C.N., Nielsen, L.B., Wibrand, F., Stride, N., Schroder, H.D., Boushel, R., Helge, J.W., Dela, F., and Hey-Mogensen, M. (2012). Biomarkers of mitochondrial content in skeletal muscle of healthy young human subjects. J Physiol *590*, 3349-3360. 10.1113/jphysiol.2012.230185.

Leary, S.C., Lyons, C.N., Rosenberger, A.G., Ballantyne, J.S., Stillman, J., and Moyes, C.D. (2003). Fiber-type differences in muscle mitochondrial profiles. American Journal of Physiology-Regulatory, Integrative and Comparative Physiology *285*, R817-R826. 10.1152/ajpregu.00058.2003.

Li, J., Van Vranken, J.G., Pontano Vaites, L., Schweppe, D.K., Huttlin, E.L., Etienne, C., Nandhikonda, P., Viner, R., Robitaille, A.M., Thompson, A.H., et al. (2020). TMTpro reagents: a set of isobaric labeling mass tags enables simultaneous proteome-wide measurements across 16 samples. Nature Methods *17*, 399-404. 10.1038/s41592-020-0781-4.

Liu, H., Sadygov, R.G., and Yates, J.R., 3rd (2004). A model for random sampling and estimation of relative protein abundance in shotgun proteomics. Analytical chemistry *76*, 4193-4201. 10.1021/ac0498563.

MacInnis, M.J., and Gibala, M.J. (2017). Physiological adaptations to interval training and the role of exercise intensity. J Physiol *595*, 2915-2930. 10.1113/jp273196.

MacInnis, M.J., Skelly, L.E., and Gibala, M.J. (2019). CrossTalk proposal: Exercise training intensity is more important than volume to promote increases in human skeletal muscle mitochondrial content. J Physiol *597*, 4111-4113. 10.1113/jp277633.

MacInnis, M.J., Zacharewicz, E., Martin, B.J., Haikalis, M.E., Skelly, L.E., Tarnopolsky, M.A., Murphy, R.M., and Gibala, M.J. (2017). Superior mitochondrial adaptations in human skeletal muscle after interval compared to continuous single-leg cycling matched for total work. The Journal of Physiology *595*, 2955-2968. 10.1113/JP272570.

Martin, W.H., 3rd, Dalsky, G.P., Hurley, B.F., Matthews, D.E., Bier, D.M., Hagberg, J.M., Rogers, M.A., King, D.S., and Holloszy, J.O. (1993). Effect of endurance training on plasma free fatty acid turnover and oxidation during exercise. The American journal of physiology *265*, E708-714. 10.1152/ajpendo.1993.265.5.E708.

Mendell, L.M. (2005). The size principle: a rule describing the recruitment of motoneurons. Journal of Neurophysiology *93*, 3024-3026. 10.1152/classicessays.00025.2005.

Miller, B.F., and Hamilton, K.L. (2012). A perspective on the determination of mitochondrial biogenesis. American journal of physiology. Endocrinology and metabolism *302*, E496-E499. 10.1152/ajpendo.00578.2011.

Morgan, T.E., Cobb, L.A., Short, F.A., Ross, R., and Gunn, D.R. (1971). Effects of Long-Term Exercise on Human Muscle Mitochondria. In Muscle Metabolism During Exercise: Proceedings of a Karolinska Institutet Symposium held in Stockholm, Sweden, September 6–9, 1970 Honorary guest: E Hohwü Christensen, B. Pernow, and B. Saltin, eds. (Springer US), pp. 87-95. 10.1007/978-1-4613-4609-8_8.

Morissette, M.P., Susser, S.E., Stammers, A.N., O'Hara, K.A., Gardiner, P.F., Sheppard, P., Moffatt, T.L., and Duhamel, T.A. (2014). Differential regulation of the fiber type-specific gene expression of the sarcoplasmic reticulum calcium-ATPase isoforms induced by exercise training. Journal of applied physiology (Bethesda, Md. : 1985) *117*, 544-555. 10.1152/japplphysiol.00092.2014.

Murgia, M., ,, Nagaraj, N., Deshmukh, A.S., Zeiler, M., Cancellara, P., Moretti, I., Reggiani, C., Schiaffino, S., and Mann, M. (2015). Single muscle fiber proteomics reveals unexpected mitochondrial specialization. EMBO Reports *16*, 387-395.

Murgia, M., Toniolo, L., Nagaraj, N., Ciciliot, S., Vindigni, V., Schiaffino, S., Reggiani, C., and Mann, M. (2017). Single Muscle Fiber Proteomics Reveals Fiber-Type- Specific Features of Human Muscle Aging Cell Reports *19*, 2396–2409.

Murphy, R.M. (2011). Enhanced technique to measure proteins in single segments of human skeletal muscle fibers: fiber-type dependence of AMPK-alpha1 and -beta1. Journal of applied physiology (Bethesda, Md. : 1985) *110*, 820-825. 10.1152/japplphysiol.01082.2010.

Neufer, P.D., Bamman, Marcas M., Muoio, Deborah M., Bouchard, C., Cooper, Dan M., Goodpaster, Bret H., Booth, Frank W., Kohrt, Wendy M., Gerszten, Robert E., Mattson, Mark P., et al. (2015). Understanding the Cellular and Molecular Mechanisms of Physical Activity-Induced Health Benefits. Cell Metabolism *22*, 4-11. https://doi.org/10.1016/j.cmet.2015.05.011.

O'Connell, J.D., Paulo, J.A., O'Brien, J.J., and Gygi, S.P. (2018). Proteome-Wide Evaluation of Two Common Protein Quantification Methods. Journal of proteome research *17*, 1934-1942. 10.1021/acs.jproteome.8b00016.

Ohlendieck, K. (2010). Proteomics of skeletal muscle differentiation, neuromuscular disorders and fiber aging. Expert review of proteomics *7*, 283-296. 10.1586/epr.10.2.

Ohlendieck, K. (2011). Skeletal muscle proteomics: current approaches, technical challenges and emerging techniques. Skeletal Muscle *1*, 1-15.

Ohlendieck, K. (2013). Proteomics of exercise-induced skeletal muscle adaptations. OA Sports Medicine *1*, 1-12.

Ørtenblad, N., Nielsen, J., Boushel, R., Söderlund, K., Saltin, B., and Holmberg, H.-C. (2018). The Muscle Fiber Profiles, Mitochondrial Content, and Enzyme Activities of the Exceptionally Well-Trained Arm and Leg Muscles of Elite Cross-Country Skiers. Frontiers in physiology *9*, 1031-1031. 10.3389/fphys.2018.01031.

Pappireddi, N., Martin, L., and Wühr, M. (2019). A Review on Quantitative Multiplexed Proteomics. Chembiochem *20*, 1210-1224. 10.1002/cbic.201800650.

Plubell, D.L., Wilmarth, P.A., Zhao, Y., Fenton, A.M., Minnier, J., Reddy, A.P., Klimek, J., Yang, X., David, L.L., and Pamir, N. (2017). Extended Multiplexing of Tandem Mass Tags (TMT) Labeling Reveals Age and High Fat Diet Specific Proteome Changes in Mouse Epididymal Adipose Tissue. Mol Cell Proteomics *16*, 873-890. 10.1074/mcp.M116.065524.

Rath, S., Sharma, R., Gupta, R., Ast, T., Chan, C., Durham, T.J., Goodman, R.P., Grabarek, Z., Haas, M.E., Hung, W.H.W., et al. (2020). MitoCarta3.0: an updated mitochondrial proteome now with sub-organelle localization and pathway annotations. Nucleic acids research. 10.1093/nar/gkaa1011.

Ritchie, M.E., Phipson, B., Wu, D., Hu, Y., Law, C.W., Shi, W., and Smyth, G.K. (2015). limma powers differential expression analyses for RNA-sequencing and microarray studies. Nucleic acids research *43*, e47. 10.1093/nar/gkv007.

Robinson, M.D., and Oshlack, A. (2010). A scaling normalization method for differential expression analysis of RNA-seq data. Genome Biology *11*, R25. 10.1186/gb-2010-11-3-r25.

Robinson, M.M., Dasari, S., Konopka, A.R., Johnson, M.L., Manjunatha, S., Esponda, R.R., Carter, R.E., Lanza, I.R., and Nair, K.S. (2017). Enhanced Protein Translation Underlies Improved Metabolic and Physical Adaptations to Different Exercise Training Modes in Young and Old Humans. Cell Metab *25*, 581-592. 10.1016/j.cmet.2017.02.009.

Sahlin, K., Mogensen, M., Bagger, M., Fernström, M., and Pedersen, P.K. (2007). The potential for mitochondrial fat oxidation in human skeletal muscle influences whole body fat oxidation during low-intensity exercise. Am J Physiol Endocrinol Metab *292*, E223-230. 10.1152/ajpendo.00266.2006.

Sale, D.G. (1987). Influence of exercise and training on motor unit activation. Exercise and sport sciences reviews *15*, 95-151.

Scalzo, R.L., Peltonen, G.L., Binns, S.E., Shankaran, M., Giordano, G.R., Hartley, D.A., Klochak, A.L., Lonac, M.C., Paris, H.L., Szallar, S.E., et al. (2014). Greater muscle protein synthesis and mitochondrial biogenesis in males compared with females during sprint interval training. Faseb j *28*, 2705-2714. 10.1096/fj.13-246595.

Schaart, G., Hesselink, R.P., Keizer, H.A., van Kranenburg, G., Drost, M.R., and Hesselink, M.K. (2004). A modified PAS stain combined with immunofluorescence for quantitative analyses of glycogen in muscle sections. Histochem Cell Biol *122*, 161-169. 10.1007/s00418-004-0690-0.

Schiaffino, S., Rossi, A.C., Smerdu, V., Leinwand, L.A., and Reggiani, C. (2015). Developmental myosins: expression patterns and functional significance. Skeletal Muscle *5*, 22. 10.1186/s13395-015-0046-6.

Schiaffino, S.a.R., C. (2011). Fiber Types in Mammalian Skeletal Muscles. Physiol Rev *91*, 1447–1531. 10.1152.

Schneider, C.A., Rasband, W.S., and Eliceiri, K.W. (2012). NIH Image to ImageJ: 25 years of image analysis. Nature Methods *9*, 671-675. 10.1038/nmeth.2089.

Scribbans, T.D., Edgett, B.A., Vorobej, K., Mitchell, A.S., Joanisse, S.D., Matusiak, J.B., Parise, G., Quadrilatero, J., and Gurd, B.J. (2014). Fibre-specific responses to endurance and low volume high intensity interval training: striking similarities in acute and chronic adaptation. PLoS One *9*, e98119. 10.1371/journal.pone.0098119.

Shaw, C.S., Swinton, C., Morales-Scholz, M.G., McRae, N.L., Erftemeyer, T., Aldous, A., Murphy, R.M., and Howlett, K.F. (2020). The impact of exercise training status on the fibre type specific abundance of proteins regulating intramuscular lipid metabolism. Journal of Applied Physiology. 10.1152/japplphysiol.00797.2019.

Shepherd, S.O., Cocks, M., Meikle, P.J., Mellett, N.A., Ranasinghe, A.M., Barker, T.A., Wagenmakers, A.J.M., and Shaw, C.S. (2017). Lipid droplet remodelling and reduced muscle ceramides following sprint interval and moderate-intensity continuous exercise training in obese males. International Journal of Obesity *41*, 1745-1754. 10.1038/ijo.2017.170.

Shepherd, S.O., Cocks, M., Tipton, K.D., Ranasinghe, A.M., Barker, T.A., Burniston, J.G., Wagenmakers, A.J., and Shaw, C.S. (2012). Preferential utilization of perilipin 2-associated intramuscular triglycerides during 1 h of moderate-intensity endurance-type exercise. Experimental physiology *97*, 970-980. 10.1113/expphysiol.2012.064592.

Shepherd, S.O., Cocks, M., Tipton, K.D., Ranasinghe, A.M., Barker, T.A., Burniston, J.G., Wagenmakers, A.J., and Shaw, C.S. (2013). Sprint interval and traditional endurance training

increase net intramuscular triglyceride breakdown and expression of perilipin 2 and 5. J Physiol *591*, 657-675. 10.1113/jphysiol.2012.240952.

Skelly, L.E., Gillen, J.B., Frankish, B.P., MacInnis, M.J., Godkin, F.E., Tarnopolsky, M.A., Murphy, R.M., and Gibala, M.J. (2021). Human skeletal muscle fiber type-specific responses to sprint interval and moderate-intensity continuous exercise: acute and training-induced changes. Journal of applied physiology (Bethesda, Md. : 1985) *130*, 1001-1014. 10.1152/japplphysiol.00862.2020.

Suriano, R., Edge, J., and Bishop, D. (2010). Effects of cycle strategy and fibre composition on muscle glycogen depletion pattern and subsequent running economy. Br J Sports Med *44*, 443-448. 10.1136/bjsm.2007.046029.

Tan, R., Nederveen, J.P., Gillen, J.B., Joanisse, S., Parise, G., Tarnopolsky, M.A., and Gibala, M.J. (2018). Skeletal muscle fiber-type-specific changes in markers of capillary and mitochondrial content after low-volume interval training in overweight women. Physiological reports *6*. 10.14814/phy2.13597.

van Loon, L.J., Greenhaff, P.L., Constantin-Teodosiu, D., Saris, W.H., and Wagenmakers, A.J. (2001). The effects of increasing exercise intensity on muscle fuel utilisation in humans. The Journal of physiology *536*, 295-304. 10.1111/j.1469-7793.2001.00295.x.

Vollestad, N.K., and Blom, P.C. (1985). Effect of varying exercise intensity on glycogen depletion in human muscle fibres. Acta Physiol Scand *125*, 395-405. 10.1111/j.1748-1716.1985.tb07735.x.

Wilson, J.M., Loenneke, J.P., Jo, E., Wilson, G.J., Zourdos, M.C., and Kim, J.S. (2012). The effects of endurance, strength, and power training on muscle fiber type shifting. J Strength Cond Res *26*, 1724-1729. 10.1519/JSC.0b013e318234eb6f.

Wyckelsma, V.L., McKenna, M.J., Serpiello, F.R., Lamboley, C.R., Aughey, R.J., Stepto, N.K., Bishop, D.J., and Murphy, R.M. (2015). Single-fiber expression and fiber-specific adaptability to short-term intense exercise training of Na+-K+-ATPase α- and β-isoforms in human skeletal muscle. Journal of Applied Physiology *118*, 699-706. 10.1152/japplphysiol.00419.2014.

Xiao, Y., Hsiao, T.H., Suresh, U., Chen, H.I., Wu, X., Wolf, S.E., and Chen, Y. (2014). A novel significance score for gene selection and ranking. Bioinformatics *30*, 801-807. 10.1093/bioinformatics/btr671.

Figure 1 Legend

a) Workflow for characterisation of pooled human skeletal muscle fibres. Single fibres from human biopsy muscle samples were taken and fibre typing was confirmed through dot blotting. After optimisation, 6 single fibres were pooled and proteins were extracted using a S-Trap™ sample processing spin column before being labelled with a TMT labelling protocol. LC-MS/MS was subsequently performed to quantify proteins for data analysis.

b) Percentage of proteins identified within the samples in comparison with the human genome. The bars display the percentage of proteins identified in the particular gene ontology cellular compartment (GOCC) group based on i) the average number of proteins identified within individual pooled samples (pink), ii) proteins identified within the entire dataset of high confidence proteins (orange) and iii) known annotated proteins in the human genome, not detected in entire single fibre dataset (grey). Identification of GOCC terms was completed using the DAVID functional annotation tool.

c) A Venn diagram displaying the proteins identified in the current study alongside two published single fibre papers. Due to differences in experimental design, and to make an appropriate comparison, Murgia et al. (2017) was filtered for young participants only with 70% valid values and Deshmukh et al. (2021) was filtered for 70% valid values.

d) Proteins identified by all three single fibre studies in Figure 1c underwent GOCC analysis. The top 5 terms of the 846 proteins identified in the intersect of Deshmukh et al., Reisman et al. and Murgia et al. are presented. The top GOCC terms and corresponding log P value were identified using the DAVID software (Huang *et al.*, 2009) and computed by a Fisher's Exact Test.

e) Multidimensional Scaling (MDS) Plot used to show the distances among fibre types for PRE exercise type I (blue) and type II (red) samples.

f) Volcano plot illustrating the fold change distribution and significance of proteins in the PRE samples between type I and type II fibres. Points were labelled based on whether they were identified as differentially expressed uniquely within our study (compared with the differentially expressed proteins identified in Deshmukh et al. 2021 and Murgia et al. 2017) or if the corresponding $-\log_{10}P$ value was greater than or equal to 5.0.

g) Heatmap displaying z-score values of differentially expressed proteins when comparing type II to type I within the PRE samples. Samples predominately cluster together by fibre type I (blue) or type II (red).

Figure 2 Legend

a) A Venn diagram displaying the number of mitochondrial proteins annotated according to the mitochondrial protein database Mitocarta 3.0 (Rath *et al.*, 2020) in the current study, alongside two published human single-fibre datasets (Deshmukh et al. 2021 and Murgia et al. 2017). Only 70% valid values pre intervention were annotated to Mitocarta 3.0.

b) Top biological processes (GOBPs) in which the identified mitochondrial proteins common to all three studies illustrated in Fig 2a are mainly involved. The bars represent $Log_{10}P$ values, where *P* represents the significance of each GOBP enriched by the mitochondrial proteins. The *P*-value was computed using DAVID software (Huang *et al.*, 2009).

c) Illustration of mitochondrial proteins that were differentially expressed between type II and type I fibres in the PRE samples. Proteins that were identified as differentially expressed following standard normalisation and mitochondrial normalisation of the data are also highlighted in green.

d) Comparison of Mean Mitochondrial Protein Expression in PRE exercise samples for type I (blue) and type II fibres (red).

e) Volcano plot illustrating the fold-change distribution of proteins in the PRE samples and the significant differences in protein expression between type I and type II fibres. Points were labelled if they were mitochondrial proteins (according to Mitocarta 3.0; (Rath *et al.*, 2020)) and identified as differentially expressed.

f) Volcano plot illustrating the fold-change distribution of proteins in the PRE samples and the significant differences in protein expression between type I and type II fibres. Points were labelled if they were mitochondrial proteins (according to Mitocarta 3.0; (Rath *et al.*, 2020)) and identified as differentially expressed following mitochondrial normalisation (Granata *et al.*, 2021).

Figure 3 Legend

a) The 8-week exercise training regime and methodology. Skeletal muscle biopsies were taken before week 1 and after week 8. Participants were randomly allocated into either the moderate-intensity continuous training (MICT) or sprint interval training (SIT) group. Grey bars indicate the number of training sessions per week. Following biopsies, muscle fibres were isolated into a single fibres. Single fibre lysates were fibre typed according to dot blotting and subsequently pooled by fibre type (six fibres). Samples then underwent LC-MS/M analysis.

b) Bar graphs displaying fold differences between the moderate-intensity continuous training (MICT) and sprint interval training (SIT) for exercise intensity (%W_{max}) and total training volume (J). Also shown are bar graphs displaying the change in blood lactate concentration (mmol•L^{-1}) and hydrogen ion (H^+) concentration (mol•L^{-1}) from pre to post exercise following the first moderate-intensity continuous exercise (MICT) and the first sprint interval exercise (SIT) session. Mean ± standard deviation ; * adjusted P value < 0.05.

c) *Histochemistry* – the effects of a single session of exercise on fibre-type specific glycogen depletion patterns in cross-sections of human vastus lateralis muscle samples collected before and after either moderate-intensity continuous exercise (MICT) or sprint interval exercise (SIT). The top panels display immunofluorescent fibre-type staining for myosin heavy chain content, with type I muscle fibres (MHC7) identified as blue and type II fibres (MHC2) identified as green. The bottom panels display serial sections that have been stained for glycogen (periodic acid-Schiff staining). Bars = 200 µm.

d) Illustration of the hierarchal recruitment pattern of type I to IIa to IIx/b skeletal muscle fibres in relation to exercise intensity. Moderate-intensity continuous exercise (MICT) is indicated in purple and sprint interval exercise (SIT) in green, with type I fibres and type II fibres in blue and red, respectively.

1266

Figure 4 Legend

a) Volcano plots illustrating the fold-change distribution of proteins that were differentially expressed in type I fibres following MICT or SIT. Proteins are coloured based on a significant fusion factor (Xiao et al., 2014) and a Log2Fold Change of > 0.2.

b) Volcano plots illustrating the fold change distribution of proteins that were differentially expressed in type II fibres following MICT or SIT. Proteins are coloured based on a significant fusion factor (Xiao et al., 2014) and a Log2Fold Change of > 0.2.

c) Venn Diagram displaying the number of proteins that were differentially expressed in type I or type II fibres following MICT, according to the fusion factor (Xiao et al., 2014).

d) Venn Diagram displaying number of proteins that were differentially expressed in type I or type II fibres following SIT, according to the fusion factor (Xiao et al., 2014).

Figure 5 Legend

a) Volcano plot illustrating the fold-change distribution of proteins between type I and II fibres in the POST MICT samples. Points were labelled based on whether they were identified as differentially expressed, according to adjusted P values from the *limma* analysis.

b) Volcano plot illustrating the fold-change distribution of proteins between type I and II fibres in the POST SIT samples. Points were labelled based on whether they were identified as differentially expressed, according to adjusted P values from the *limma* analysis.

c) Venn Diagrams displaying number of proteins identified as higher in type I or type II fibres for both exercise types, with the proteins that appear in both datasets seen in the overlap. Individual proteins are listed in supplemental Table 5, Tab 3.

d) Venn Diagram displaying the number of proteins that were differentially expressed between type I and type II fibres in the PRE samples (n=23 participants), compared with the number of differentially expressed proteins between type I and type II fibres in the POST MICT (n = 11) and SIT samples (n=12).

e) *EnrichPlot* dot plot results of protein expression in type I vs type II fibres for the POST MICT and SIT samples. Pathway terms were identified using WikiPathways. The top 15 terms according to adjusted P-values are displayed. Red dots identify pathway terms found higher in type II fibres, while blue dots indicate pathway terms found higher in type I fibres. Saturation of each colour is proportional to the average log2 fold change for each exercise and fibre group. The size of each dot indicates how many proteins correspond to each pathway term. For all proteins, the corresponding log_2 fold change and P-values from the differential expression analysis were used. All terms identified can be found in supplemental Table 5, Tab 5.

f) *ClusterProfiler* network plot using differentially expressed (adjusted P value < 0.05) terms. Pathway terms were identified using WikiPathways. Colours indicate in which exercise and fibre group the proteins in that WikiPathway term were found. The size of each circle indicates how many proteins corresponded to each term. The displayed terms were manually selected for readability of the figure. All terms identified can be found in supplemental Table 5, Tab 6.

Figure 6 Legend

a) A representative images of a skeletal muscle samples analysed using transmission electron microscopy (TEM) pre- and post-training for both MICT and SIT. Note the difference in the abundance of mitochondria. Bars = 0.5 µm

b) Violin plots of change (Δ) in mitochondrial volume density (% $Mito_{VD}$) from pre to post training following moderate-intensity continuous training (MICT - purple) and sprint interval training (SIT - green).

c) Violin plots of change (Δ) in citrate synthase activity (CS; $mol.h^{-1}.kg\ protein^{-1}$) from pre to post training following moderate-intensity continuous training (MICT - purple) and sprint interval training (SIT - green).

d) Scaled profile plots showing the relative abundance of mitochondrial proteins (grey) pre and post exercise in the MICT (purple) and SIT (green) groups for each fibre type, and the mean relative abundance (black) of the proteins in each group.

Data in d & e are shown as Δ mean z-score. * indicates P values for significance (*: P <= 0.01, **: P <= 0.001, ***: P <= 0.0001, ****: P <= 0.00001) by paired t-test from pre to post training.

1335

Figure 7 Legend

a) Scaled profile plots with the application of mitochondrial normalisation showing changes in the relative abundance of mitochondrial proteins (grey) pre and post training in the MICT and SIT groups for each fibre type. The mean of each group is indicated by the black line. Data is shown as Δ mean z-score.

b) Scaled profile plots with the application of mitochondrial normalisation showing changes in the relative abundance of the subunits in each of the oxidative phosphorylation (OXPHOS) complexes (CI to CV), as well as the mitochondrial ribosome, in type I and type II fibre types in response to both types of training (MICT and SIT). The mean of each group (all proteins identified in each pathway using MitoCarta 3.0) is indicated by the black line. Data is shown as Δ mean z-score.
* indicates P value for significance (*: $P \leq 0.01$, **: $P \leq 0.001$, ***: $P \leq 0.0001$, ****: $P \leq 0.00001$) based on a paired t-test of the pre to post training values.

c) Scaled profile plots with the application of mitochondrial normalisation showing changes in the relative abundance of proteins involved in Fatty Acid Oxidation, the tricarboxylic acid cycle, and mitochondrial dynamics (all proteins identified in pathway using MitoCarta 3.0) in type I and type II fibre types in response to both types of training (MICT and SIT). The mean of each group is indicated by the black line. Data is shown as Δ mean z-score. * indicates P value for significance (*: $P \leq 0.01$, **: $P \leq 0.001$, ***: $P \leq 0.0001$, ****: $P \leq 0.00001$) based on a paired t-test of the pre to post training values.

d) Heatmap displaying z-score values of protein subunits of the OXPHOS complexes, as well as the mitochondrial ribosome, in each of the two training groups (MICT and SIT), in type I and type II fibre types pre and post training, with the application of mitochondrial normalisation.

Supplemental Figure 1 Legend

a) Heatmap displaying z-score values of protein subunits of the OXPHOS complexes, as well as the mitochondrial ribosome, in each of the two training groups (MICT and SIT), in type I and type II fibre types pre and post training, without the application of mitochondrial normalisation.

b) Scaled profile plots without the application of mitochondrial normalisation showing changes in the relative abundance of the subunits in each of the oxidative phosphorylation (OXPHOS) complexes (CI to CV), as well as the mitochondrial ribosome, in type I and type II fibre types in response to both types of training (MICT and SIT). The mean of each group (all proteins identified in each pathway using MitoCarta 3.0) is indicated by the black line. Data is shown as Δ mean z-score. * indicates P value for significance (*: $P \leq 0.01$, **: $P \leq 0.001$, ***: $P \leq 0.0001$, ****: $P \leq 0.00001$) based on a paired t-test of the pre to post training values.

c) Scaled profile plots without the application of mitochondrial normalisation showing changes in the relative abundance of proteins involved in Fatty Acid Oxidation, the tricarboxylic acid cycle, and mitochondrial dynamics (all proteins identified in pathway using MitoCarta 3.0) in type I and type II fibre types in response to both types of training (MICT and SIT). The mean of each group is indicated by the black line. Data is shown as Δ mean z-score. * indicates P value for significance (*: $P \leq 0.01$, **: $P \leq 0.001$, ***: $P \leq 0.0001$, ****: $P \leq 0.00001$) based on a paired t-test of the pre to post training values.

Supplementary Figure 2 Legend

a) Number of proteins quantified in the training study dataset by our proteomic workflow in all pooled single-fibre samples. Samples are arranged according to TMT batches (A-H). Samples are labelled according to participant ID (Z to A), training type (S or M), Biopsy time (pre or post), and fibre type (I or II))

b) Reproducibility of protein intensities (intensity-based absolute quantification; IBAQ) for replicates of type I skeletal muscle fibre samples. Core mitochondrial proteins (OXPHOS – NDUFA8, SDHA, URCRC2, COX5B, ATP5B, IDH3B and CKM) are highlighted in yellow, in addition to sarcomeric proteins (MYH 7 (blue), ACTA1 (orange)).

c) Reproducibility of protein intensities (intensity-based absolute quantification; IBAQ) for replicates of type II skeletal muscle fibre samples. Core mitochondrial proteins (OXPHOS – NDUFA8, SDHA, URCRC2, COX5B, ATP5B, IDH3B and CKM) are highlighted in yellow, in addition to MYH2 (green).

d) Relative abundance of myosin heavy chains (MYH) in type I samples pooled by dot blotting, according to the percentage of the MYH7 (blue = type I), MYH2 (red = type-IIa) MYH1 (brown = type-IIx), and MYH4 (purple = type IIb) protein isoforms detected.

e) Relative abundance of myosin heavy chains (MYH) in type II samples pooled by dot blotting, according to the percentage of the MYH7 (blue = type I), MYH2 (red = type-IIa) MYH1 (brown = type-IIx), and MYH4 (purple = type IIb) protein isoforms detected.

f) Study recruitment flow chart and final group sizes for the groups that completed 8 weeks of moderate-intensity interval training (MICT) or sprint interval training (SIT). Following the initial recruitment of 28 participants, 2 men from each group dropped out of the study due to time constraints and one fibrotic muscle sample was removed from the MICT group muscle analysis.

g) Sampling strategy when using a 96-well plate to best accommodate for possible reporter ion interferences. Reporter ion interference (RII) targets were classified according to a typical product data sheet for 16-plex TMTpro Label Reagents from ThermoFisher Scientific.

h) Hierarchical visualisation of the statistical comparisons performed in this study.

Description of Additional Supplementary Files

File name: Supplementary Table 1

Description: Participant characteristics, Raw intensities for all proteomic data, and log intensities for all identified proteins in all samples following the normalisation described in the methods. Data also includes gene ontology cellular compartment (GOCC) analysis for pooled single fibre analysis for percentage of cellular compartment identified (shown in Figure 1b) and the top 5 GOCC and corresponding $\log_{10}$ P value identified using the DAVID software for proteins identified by key single fibre proteomic studies (shown in Figure 1c). Further analysis includes the protein lists presented in the Venn diagram of Figure 1c for identified proteins within the current study, along with the studies of Deshmukh et al. and Murgia et al. (Tab 5), along with the top GOCC terms for the common proteins identified in all 3 studies (Fig 1d, Tab 6). Statistical analysis is lastly presented via logged intensities of proteins within the PRE type I and type II fibre samples. The table also displays calculations completed to calculate the 'Fusion Factor' used in Deshmukh et al. (2021) and the corresponding significance. Further detail is provided in the legend tab of the linked Excel file.

File name: Supplementary Table 2

Description: The list of mitochondrial proteins (according to Mitocarta 3.0) in common to all previous single fibre human studies pre intervention. Further analysis is presented in the table output by the DAVID software to identify top gene ontology biological processes (GOBP) groups of the mitochondrial proteins identified in over 70% of the total sample in all three studies listed (Deshmukh et al., Murgia et al., and the current study). Further analysis is presented with the average of all mitochondrial proteins in each individual. The mean of averages were calculated and compared between PRE training type I fibres and type II fibres. Mitochondrial protein expression (MPE) calculation is subsequently presented for identified mitochondrial proteins within the study in each comparison. Data normalised for mitochondrial content for identified mitochondrial proteins within the study for the PRE type I vs II comparison and presented in the volcano plots (Figure 2f). Further detail provided in the legend tab of the linked Excel file.

File name: Supplementary Table 3

Description: Fold Difference from Pre to Post exercise for blood concentration of H^+ and lactate results.

File name: Supplementary Table 4

Description: The normalised Data (Log2) with *limma* and Fusion Factor calculations for MICT Type I and Type II - PRE vs POST. In addition, Normalised Data (Log_2 with *limma* and Fusion Factor Calculations for SIT type I & type II - PRE vs POST. Proteins identified in type I vs type II fibres POST MICT and corresponding GO Biological Processes results. Parallel analysis is presented for POST SIT. Further detail is provided in the legend tab of the linked Excel file.

File name: Supplementary Table 5

Description: Log intensities for type I versus type II fibres in POST MICT and SIT samples following normalisation. GO Enrichment (Biological Processes) completed with DAVID on the common and unique MICT and SIT proteins identified when comparing Post I vs II samples. Further corresponding GOBP analysis is also made proteins identified as differentially expressed between type I and II fibres in the PRE samples. Further enrichment analysis is undertaken via WikiPathways enrichment analysis and Network analysis of differences in protein abundance between type I & type II fibres in the POST samples for MICT & SIT (analysed separately), using enrichplot & clusterprofiler on the *limma* results displayed in Tab 1 and 2 of this file. Further detail provided in the legend tab of the linked Excel file.

File name: Supplementary Table 6

Description: Differences from Pre to Post training for Mitochondria Volume Density (%) and Citrate Synthase activity ($mol \bullet h^{-1} \bullet kg\ protein^{-1}$) for MICT & SIT. Analysis presented for scaled intensities (z-scores) and means for known mitochondrial proteins for all samples following standard normalisation. Scaled means for each complex in each sample group are also presented in addition to the mean change for each comparison of training and fibre type. Further detail is provided in the legend tab of the linked Excel file.

File name: Supplementary Table 7

Description: Scaled intensities and means for known mitochondrial proteins for all samples following mitochondrial normalisation. Protein functional classes and metabolic pathways presented with the scaled means (z-scores) for each functional group (defined by MitoCarta

3.0) in each sample group in addition to the mean change for each comparison of training and fibre type with mitochondrial normalisation applied. Further detail provided in the legend tab of the linked Excel file.

File name: Supplementary Table 8

Description: Protein functional classes and metabolic pathways presented with the scaled means (z-scores) for each functional group (defined by MitoCarta 3.0) in each sample group in addition to the mean change for each comparison of training and fibre type. Further detail is provided in the legend tab of the linked Excel file.

File name: Supplementary Table 9

Description: The number of proteins quantified in the training study dataset by our proteomic workflow in all pooled single-fibre samples. Raw TMT Batch ID is presented and arranged according to TMT batches (A-H). Samples are labelled according to participant ID (Z-C), training type (S for SIT or M for MICT), training time (pre or post) and fibre type (I or II). In addition, reliability between replicates is presented - List of Intensity reported by intensity-based absolute quantification (IBAQ) for replicates and corresponding gene names of pooled type I fibres (n = 6 fibres) and type II fibres. Furthermore, the relative TMT intensity and percentage abundance of myosin heavy chains (MYH) for type I and type II samples pooled by dot blotting is presented.

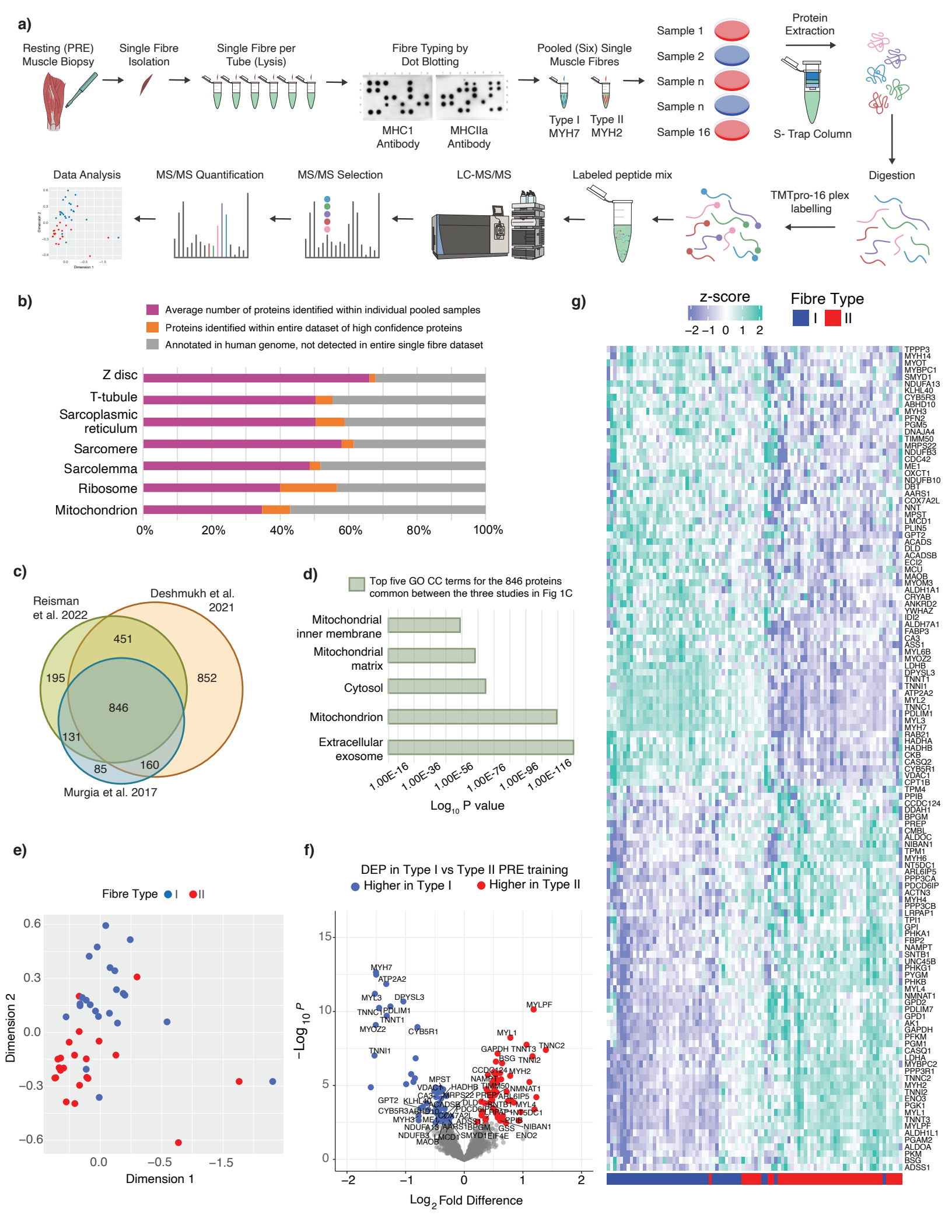
a)
Resting (PRE) Muscle Biopsy
Single Fibre Isolation
Single Fibre per Tube (Lysis)
Fibre Typing by Dot Blotting
MHC1 Antibody
MHCIIa Antibody
Pooled (Six) Single Muscle Fibres
Type I MYH7
Type II MYH2
Sample 1
Sample 2
Sample n
Sample n
Sample 16
Protein Extraction
S- Trap Column
Digestion
TMTpro-16 plex labelling
Labeled peptide mix
LC-MS/MS
MS/MS Selection
MS/MS Quantification
Data Analysis
b)
Average number of proteins identified within individual pooled samples
Proteins identified within entire dataset of high confidence proteins
Annotated in human genome, not detected in entire single fibre dataset
Z disc
T-tubule
Sarcoplasmic reticulum
Sarcomere
Sarcolemma
Ribosome
Mitochondrion
0%
20%
40%
60%
80%
100%
c)
Reisman et al. 2022
Deshmukh et al. 2021
Murgia et al. 2017
195
451
852
846
131
85
160
d)
Top five GO CC terms for the 846 proteins common between the three studies in Fig 1C
Mitochondrial inner membrane
Mitochondrial matrix
Cytosol
Mitochondrion
Extracellular exosome
1.00E-16
1.00E-36
1.00E-56
1.00E-76
1.00E-96
1.00E-116
Log10 P value
e)
Fibre Type I II
Dimension 2
Dimension 1
0.6
0.3
0.0
−0.3
−0.6
0.0
−0.5
−1.5
f)
DEP in Type I vs Type II PRE training
Higher in Type I
Higher in Type II
−Log10 P
Log2 Fold Difference
MYH7
ATP2A2
MYL3
DPYSL3
TNNC1
PDLIM1
TNNT1
MYOZ2
CYB5R1
TNNI1
MYLPF
MYL1
GAPDH
TNNT3
TNNC2
BSG
TNNI2
CCDC124
MYH2
NAMPT
MPST
VDAC1
HADHB
TMM50
NMNAT1
CA3
MRPS22
PREP
ARL6IP5
GPT2
KLHL40
ACADSB
DLD
SNTB1
MYL4
CYB5R3
ABHD10
PDCD6IP
LRPAP1
PDC1
MYH3
ME1
COX7A2L
ADSS1
PPIB
NDUFA13
AARS1
BPGM
GSS
NIBAN1
NDUFB3
LMCD1
SMYD1
EIF4E
ENO2
MAOB
g)
z-score
−2 −1 0 1 2
Fibre Type
I
II
TPPP3
MYH14
MYOT
MYBPC1
SMYD1
NDUFA13
KLHL40
CYB5R3
ABHD10
MYH3
PFN2
PGM5
DNAJA4
TIMM50
MRPS22
NDUFB3
CDC42
ME1
OXCT1
NDUFB10
DBT
AARS1
COX7A2L
NNT
MPST
LMCD1
PLIN5
GPT2
ACADS
DLD
ACADSB
ECI2
MCU
MAOB
MYOM3
ALDH1A1
CRYAB
ANKRD2
YWHAZ
IDI2
ALDH7A1
FABP3
CA3
ASS1
MYL6B
MYOZ2
LDHB
DPYSL3
TNNT1
TNNI1
ATP2A2
MYL2
TNNC1
PDLIM1
MYL3
MYH7
RAB21
HADHA
HADHB
CKB
CASQ2
CYB5R1
VDAC1
CPT1B
TPM4
PPIB
CCDC124
DDAH1
BPGM
PREP
CMBL
ALDOC
NIBAN1
TPM1
MYH6
NT5DC1
ARL6IP5
PPP3CA
PDCD6IP
ACTN3
MYH4
PPP3CB
LRPAP1
TPI1
GPI
PHKA1
FBP2
NAMPT
SNTB1
UNC45B
PHKG1
PYGM
PHKB
MYL4
NMNAT1
GPD2
PDLIM7
GPD1
AK1
GAPDH
PFKM
PGM1
CASQ1
LDHA
MYBPC2
PPP3R1
TNNC2
MYH2
TNNI2
ENO3
PGK1
MYL1
TNNT3
MYLPF
ALDH1L1
PGAM2
ALDOA
PKM
BSG
ADSS1

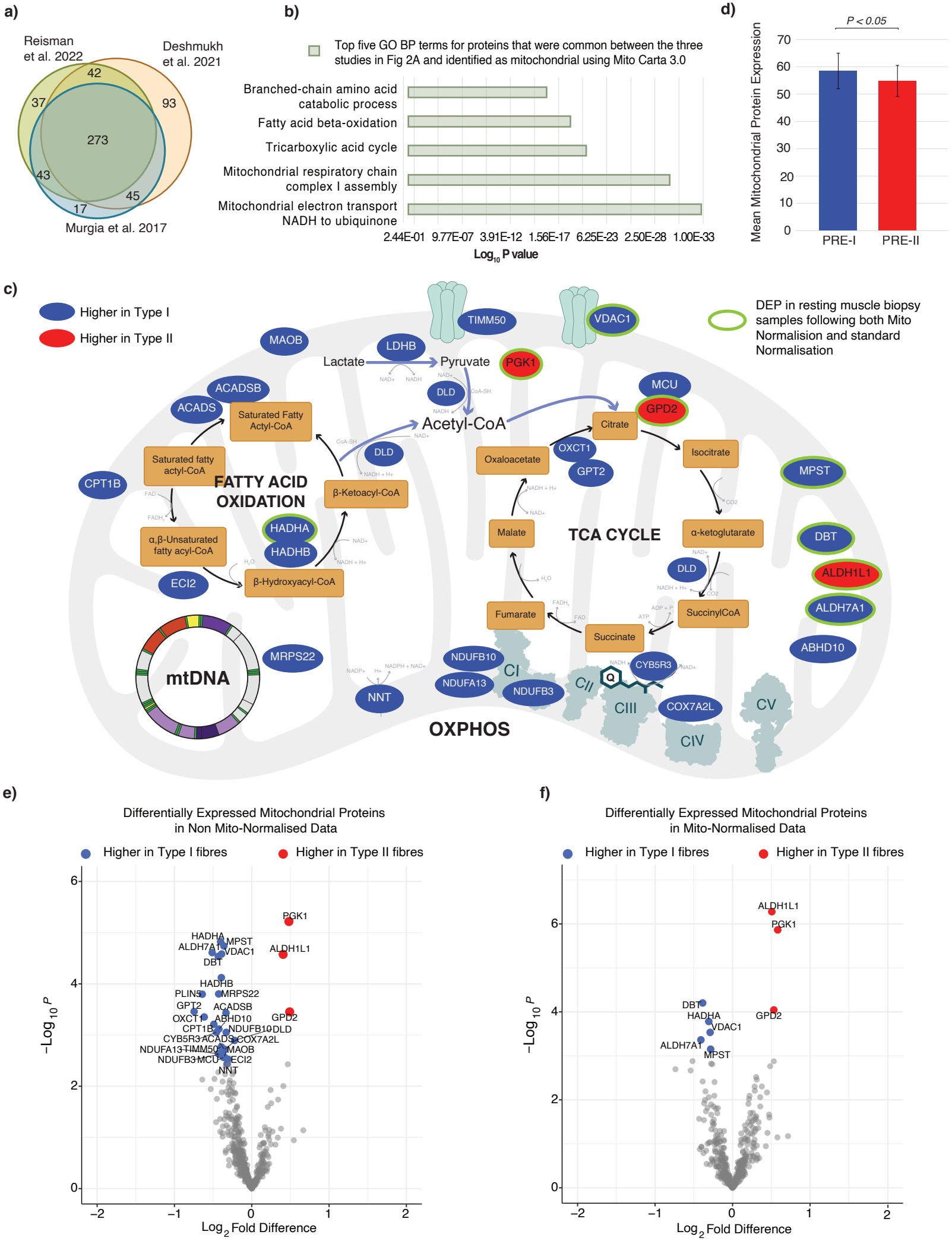
a)
Reisman et al. 2022
Deshmukh et al. 2021
Murgia et al. 2017
42
37
93
273
43
45
17
b)
Top five GO BP terms for proteins that were common between the three studies in Fig 2A and identified as mitochondrial using Mito Carta 3.0
Branched-chain amino acid catabolic process
Fatty acid beta-oxidation
Tricarboxylic acid cycle
Mitochondrial respiratory chain complex I assembly
Mitochondrial electron transport NADH to ubiquinone
2.44E-01 9.77E-07 3.91E-12 1.56E-17 6.25E-23 2.50E-28 1.00E-33
Log10 P value
d)
P < 0.05
Mean Mitochondrial Protein Expression
70
60
50
40
30
20
10
0
PRE-I
PRE-II
c)
Higher in Type I
Higher in Type II
DEP in resting muscle biopsy samples following both Mito Normalisation and standard Normalisation
TIMM50
VDAC1
MAOB
LDHB
Lactate
Pyruvate
PGK1
DLD
Acetyl-CoA
MCU
GPD2
ACADSB
ACADS
Saturated Fatty Actyl-CoA
Citrate
Isocitrate
Saturated fatty actyl-CoA
Oxaloacetate
OXCT1
GPT2
MPST
CPT1B
FATTY ACID OXIDATION
β-Ketoacyl-CoA
HADHA
HADHB
α,β-Unsaturated fatty acyl-CoA
Malate
TCA CYCLE
α-ketoglutarate
DBT
ECI2
β-Hydroxyacyl-CoA
ALDH1L1
ALDH7A1
Fumarate
SuccinylCoA
Succinate
ABHD10
mtDNA
MRPS22
NDUFB10
CI
CYB5R3
NDUFA13
NDUFB3
CII
CIII
COX7A2L
CV
NNT
CIV
OXPHOS
e)
Differentially Expressed Mitochondrial Proteins in Non Mito-Normalised Data
Higher in Type I fibres
Higher in Type II fibres
PGK1
HADHA
MPST
ALDH7A1
VDAC1
ALDH1L1
DBT
HADHB
PLIN5
MRPS22
GPT2
ACADSB
OXCT1
ABHD10
GPD2
CPT1B
NDUFB10
DLD
CYB5R3
ACADS
COX7A2L
NDUFA13
TIMM50
MAOB
NDUFB3
MCU
ECI2
NNT
−Log10 P
Log2 Fold Difference
f)
Differentially Expressed Mitochondrial Proteins in Mito-Normalised Data
Higher in Type I fibres
Higher in Type II fibres
ALDH1L1
PGK1
DBT
HADHA
GPD2
VDAC1
ALDH7A1
MPST
−Log10 P
Log2 Fold Difference

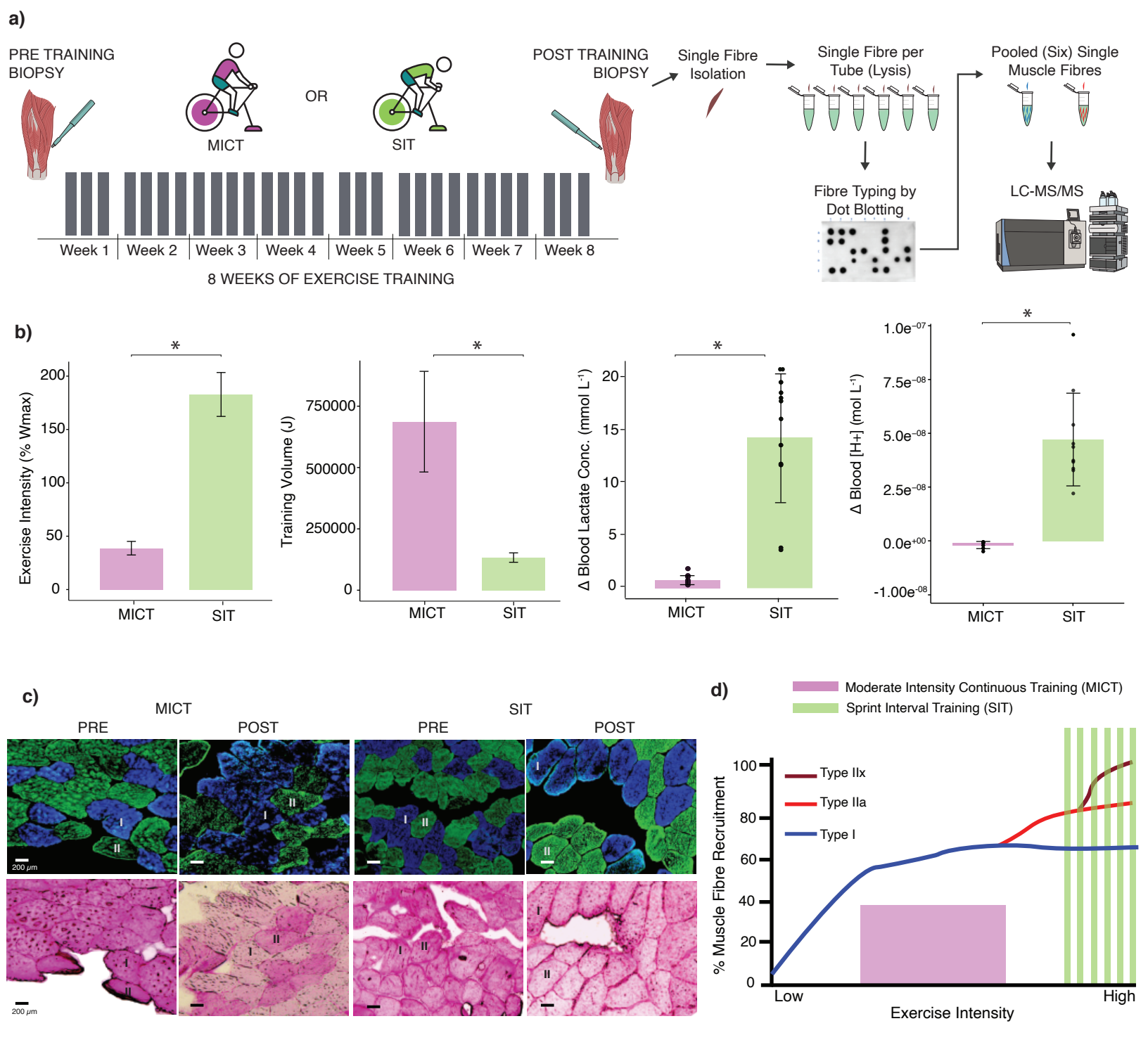
a)
PRE TRAINING BIOPSY
MICT
OR
SIT
POST TRAINING BIOPSY
Single Fibre Isolation
Single Fibre per Tube (Lysis)
Pooled (Six) Single Muscle Fibres
Fibre Typing by Dot Blotting
LC-MS/MS
Week 1
Week 2
Week 3
Week 4
Week 5
Week 6
Week 7
Week 8
8 WEEKS OF EXERCISE TRAINING
b)
Exercise Intensity (% Wmax)
Training Volume (J)
Δ Blood Lactate Conc. (mmol L⁻¹)
Δ Blood [H+] (mol L⁻¹)
MICT
SIT
c)
MICT
SIT
PRE
POST
200 μm
d)
Moderate Intensity Continuous Training (MICT)
Sprint Interval Training (SIT)
Type IIx
Type IIa
Type I
% Muscle Fibre Recruitment
Low
High
Exercise Intensity

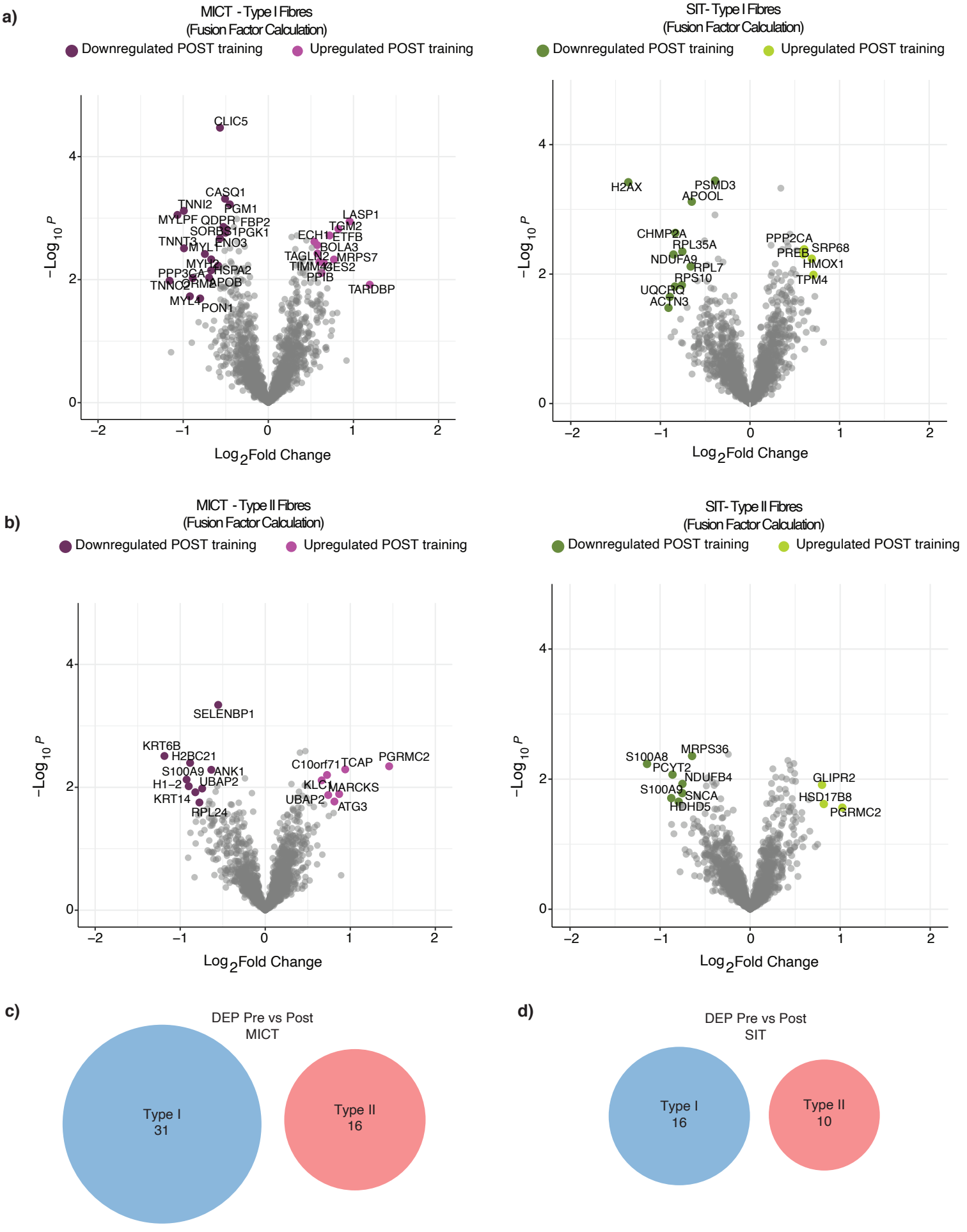
a)
MICT - Type I Fibres
(Fusion Factor Calculation)
Downregulated POST training
Upregulated POST training
CLIC5
CASQ1
TNNI2
PGM1
MYLPF
QDPR
FBP2
SORBS1
PGK1
TNNT3
ENO3
MYL1
MYH2
HSPA2
PPP3CA
TNNC2
ORMDL
APOB
MYL4
PON1
LASP1
TGM2
ECH1
ETFB
BOLA3
TAGLN2
MRPS7
TIMM44
ES2
PPIB
TARDBP
−Log10 P
Log2Fold Change
SIT- Type I Fibres
(Fusion Factor Calculation)
Downregulated POST training
Upregulated POST training
H2AX
PSMD3
APOOL
CHMP2A
RPL35A
NDUFA9
RPL7
RPS10
UQCRQ
ACTN3
PPP2CA
PREB
SRP68
HMOX1
TPM4
−Log10 P
Log2Fold Change
b)
MICT - Type II Fibres
(Fusion Factor Calculation)
Downregulated POST training
Upregulated POST training
SELENBP1
KRT6B
H2BC21
S100A9
ANK1
H1−2
UBAP2
KRT14
RPL24
C10orf71
TCAP
PGRMC2
KLC1
MARCKS
UBAP2
ATG3
−Log10 P
Log2Fold Change
SIT- Type II Fibres
(Fusion Factor Calculation)
Downregulated POST training
Upregulated POST training
S100A8
MRPS36
PCYT2
NDUFB4
S100A9
SNCA
HDHD5
GLIPR2
HSD17B8
PGRMC2
−Log10 P
Log2Fold Change
c)
DEP Pre vs Post
MICT
Type I
31
Type II
16
d)
DEP Pre vs Post
SIT
Type I
16
Type II
10

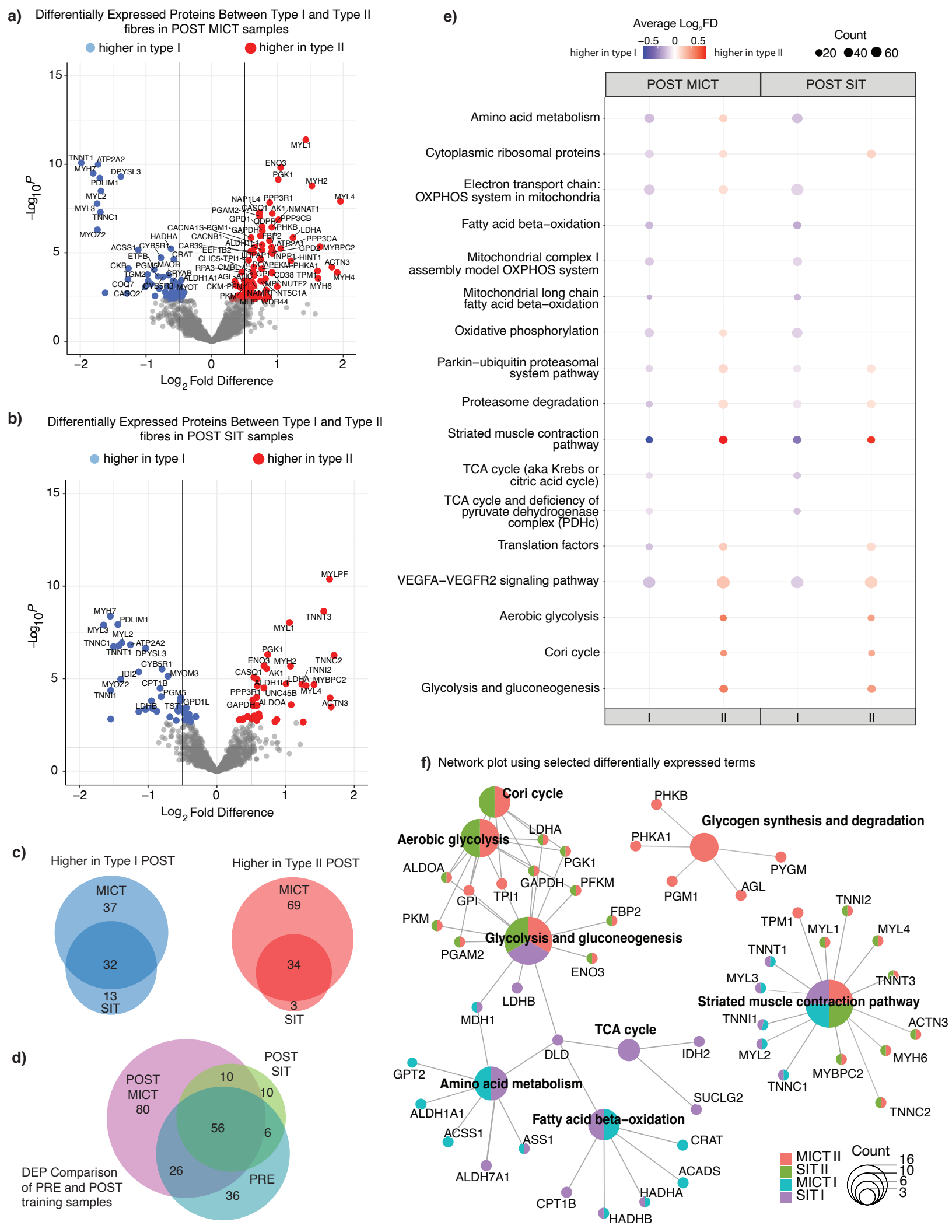
a)
Differentially Expressed Proteins Between Type I and Type II fibres in POST MICT samples
higher in type I
higher in type II
−Log10P
Log2 Fold Difference
b)
Differentially Expressed Proteins Between Type I and Type II fibres in POST SIT samples
higher in type I
higher in type II
−Log10P
Log2 Fold Difference
c)
Higher in Type I POST
MICT
37
32
13
SIT
Higher in Type II POST
MICT
69
34
3
SIT
d)
POST MICT
80
POST SIT
10
10
56
6
26
36
PRE
DEP Comparison of PRE and POST training samples
e)
Average Log2FD
−0.5 0 0.5
higher in type I
higher in type II
Count
20 40 60
POST MICT
POST SIT
Amino acid metabolism
Cytoplasmic ribosomal proteins
Electron transport chain: OXPHOS system in mitochondria
Fatty acid beta−oxidation
Mitochondrial complex I assembly model OXPHOS system
Mitochondrial long chain fatty acid beta−oxidation
Oxidative phosphorylation
Parkin−ubiquitin proteasomal system pathway
Proteasome degradation
Striated muscle contraction pathway
TCA cycle (aka Krebs or citric acid cycle)
TCA cycle and deficiency of pyruvate dehydrogenase complex (PDHc)
Translation factors
VEGFA−VEGFR2 signaling pathway
Aerobic glycolysis
Cori cycle
Glycolysis and gluconeogenesis
I
II
I
II
f)
Network plot using selected differentially expressed terms
Cori cycle
Aerobic glycolysis
Glycogen synthesis and degradation
Glycolysis and gluconeogenesis
Striated muscle contraction pathway
TCA cycle
Amino acid metabolism
Fatty acid beta−oxidation
MICT II
SIT II
MICT I
SIT I
Count
16
10
6
3

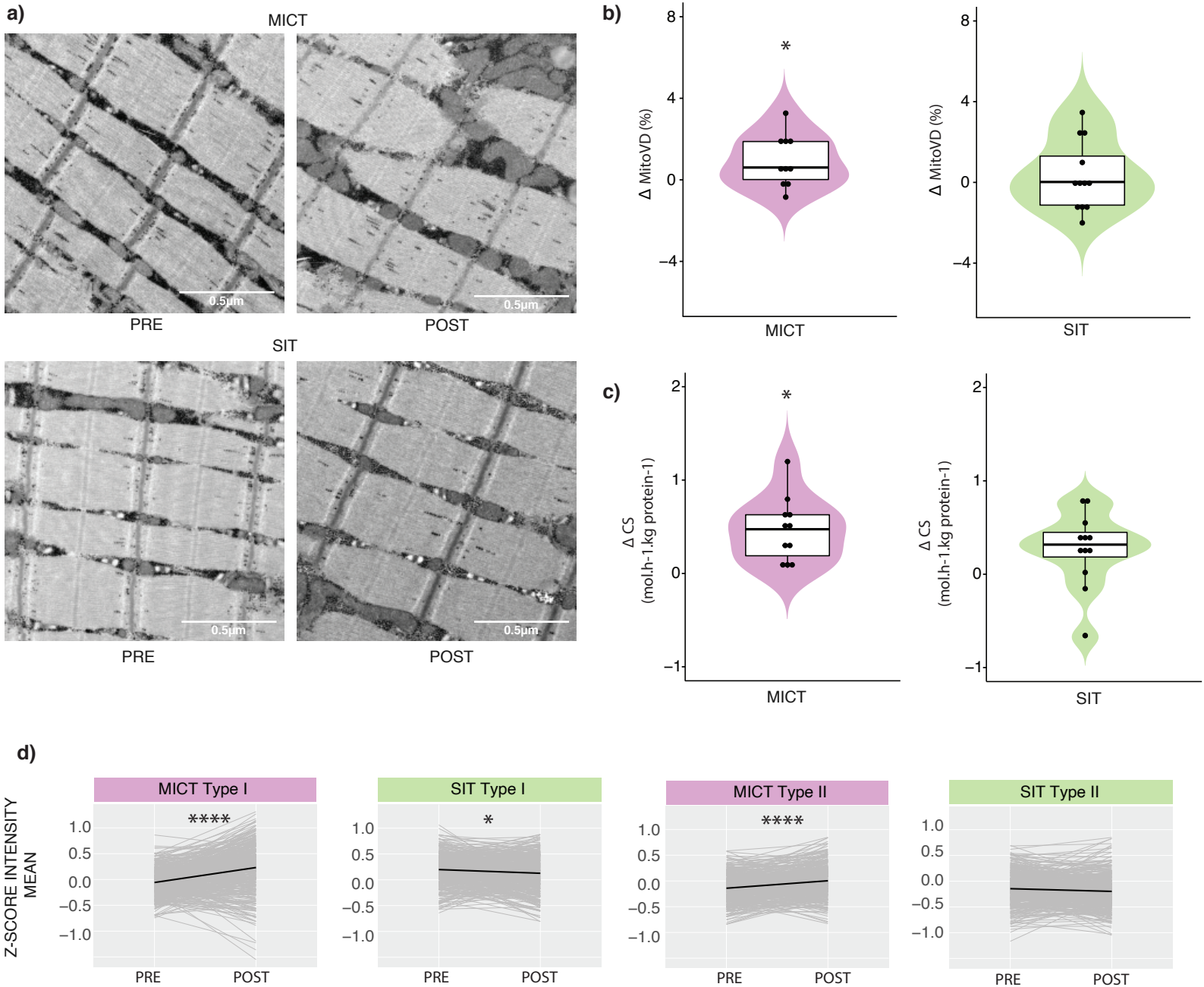
a)
MICT
0.5µm
0.5µm
PRE
POST
SIT
0.5µm
0.5µm
PRE
POST
b)
Δ MitoVD (%)
8
4
0
−4
*
MICT
SIT
c)
Δ CS
(mol.h-1.kg protein-1)
2
1
0
−1
*
MICT
SIT
d)
Z-SCORE INTENSITY
MEAN
MICT Type I
SIT Type I
MICT Type II
SIT Type II
1.0
0.5
0.0
−0.5
−1.0
****
*
****
PRE
POST

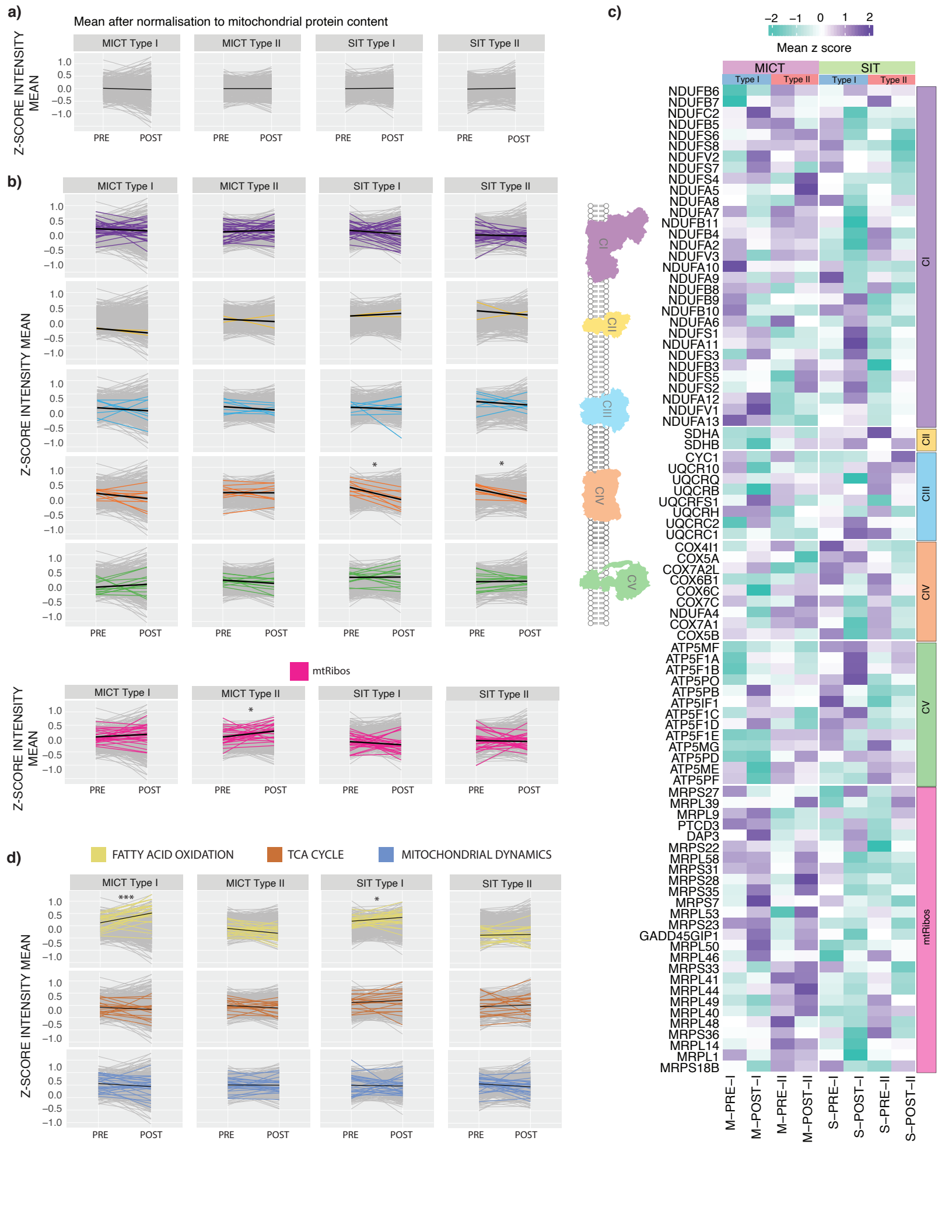
a)
Mean after normalisation to mitochondrial protein content
MICT Type I
MICT Type II
SIT Type I
SIT Type II
Z-SCORE INTENSITY MEAN
PRE
POST
b)
mtRibos
d)
FATTY ACID OXIDATION
TCA CYCLE
MITOCHONDRIAL DYNAMICS
c)
Mean z score
MICT
SIT
Type I
Type II
CI
CII
CIII
CIV
CV
mtRibos
M–PRE–I
M–POST–I
M–PRE–II
M–POST–II
S–PRE–I
S–POST–I
S–PRE–II
S–POST–II

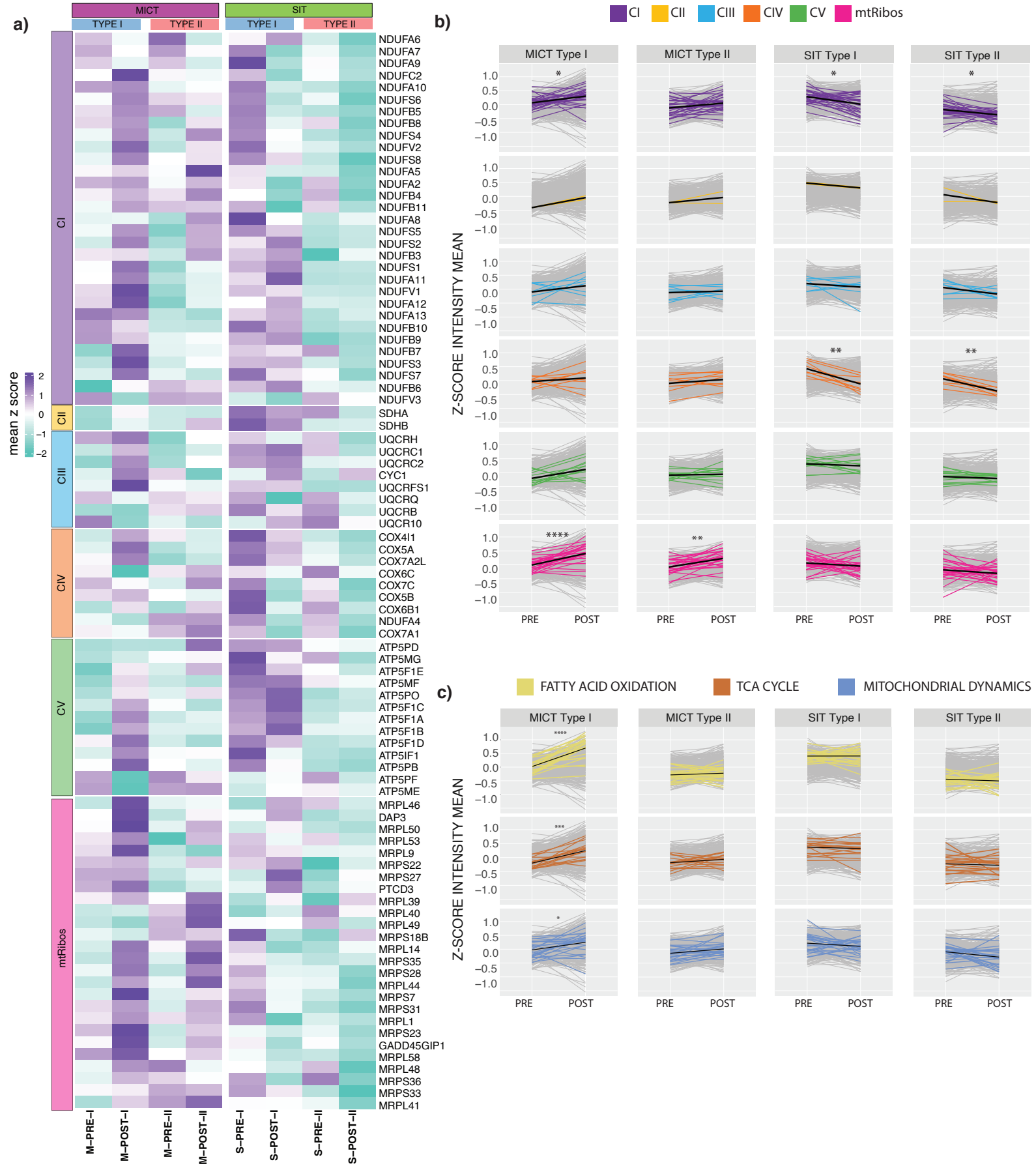
a)
MICT
SIT
TYPE I
TYPE II
CI
CII
CIII
CIV
CV
mtRibos
mean z score
M–PRE–I
M–POST–I
M–PRE–II
M–POST–II
S–PRE–I
S–POST–I
S–PRE–II
S–POST–II
b)
CI
CII
CIII
CIV
CV
mtRibos
MICT Type I
MICT Type II
SIT Type I
SIT Type II
Z-SCORE INTENSITY MEAN
PRE
POST
c)
FATTY ACID OXIDATION
TCA CYCLE
MITOCHONDRIAL DYNAMICS

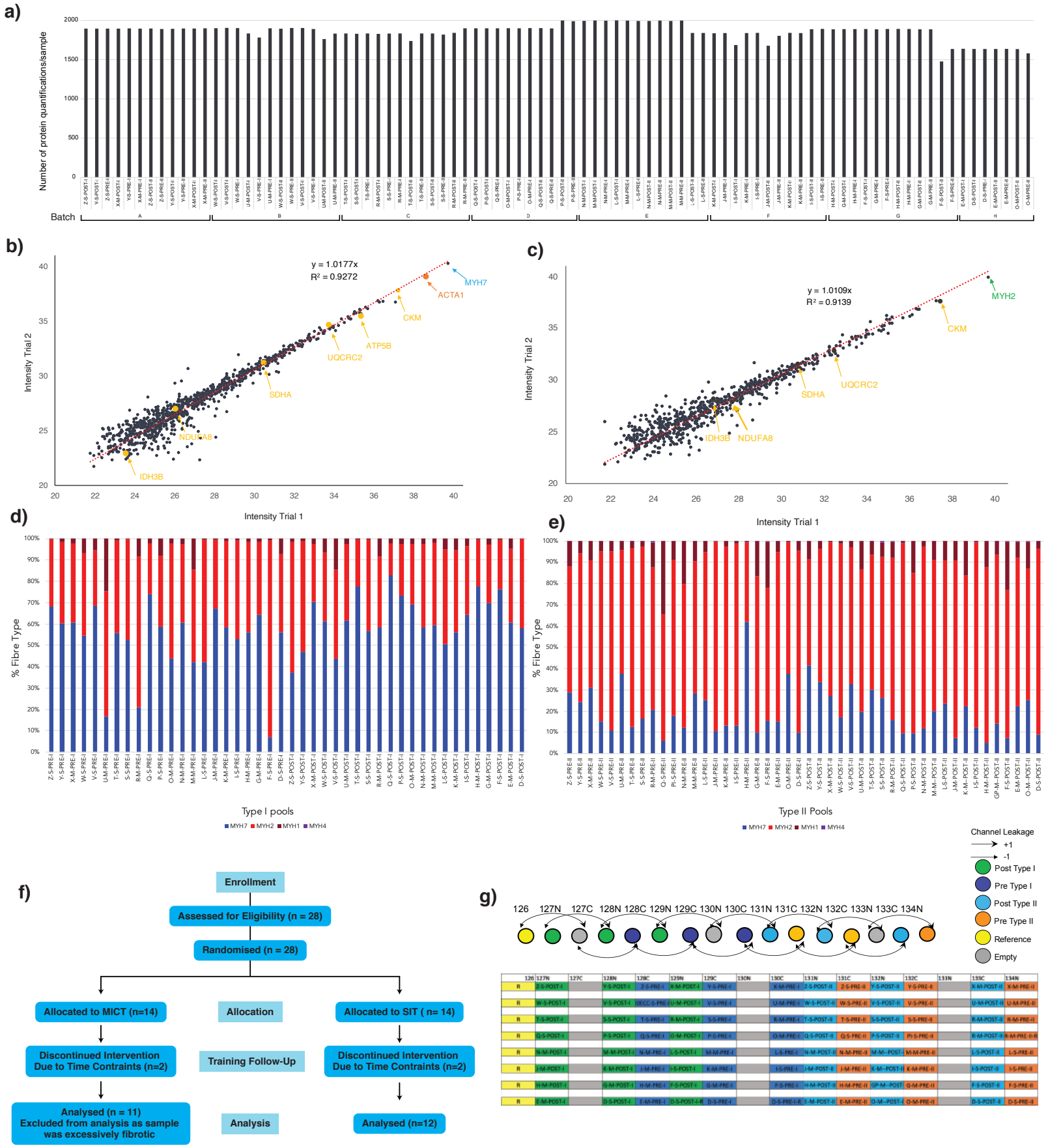
a)
Number of protein quantifications/sample
Batch
b)
y = 1.0177x
R² = 0.9272
MYH7
ACTA1
CKM
ATP5B
UQCRC2
SDHA
NDUFA8
IDH3B
Intensity Trial 2
Intensity Trial 1
c)
y = 1.0109x
R² = 0.9139
MYH2
CKM
UQCRC2
SDHA
IDH3B
NDUFA8
Intensity Trial 2
Intensity Trial 1
d)
% Fibre Type
Type I pools
MYH7 MYH2 MYH1 MYH4
e)
% Fibre Type
Type II Pools
MYH7 MYH2 MYH1 MYH4
Channel Leakage
+1
-1
Post Type I
Pre Type I
Post Type II
Pre Type II
Reference
Empty
f)
Enrollment
Assessed for Eligibility (n = 28)
Randomised (n = 28)
Allocated to MICT (n=14)
Allocation
Allocated to SIT (n= 14)
Discontinued Intervention Due to Time Contraints (n=2)
Training Follow-Up
Discontinued Intervention Due to Time Contraints (n=2)
Analysed (n = 11) Excluded from analysis as sample was excessively fibrotic
Analysis
Analysed (n=12)
g)
126 127N 127C 128N 128C 129N 129C 130N 130C 131N 131C 132N 132C 133N 133C 134N
h)
MICT
SIT
Pre Training
Post Training
Type I
Type II